

# Trapping of Dust by Coherent Vortices in the Solar Nebula

Pierre-Henri CHAVANIS<sup>1,2</sup>

<sup>1</sup>Laboratoire de Physique Quantique, Université Paul Sabatier, 118 route de Narbonne 31062 Toulouse, France

<sup>2</sup>Istituto di Cosmogeofisica, Corso Fiume 4, 10133 Torino, Italia

May 7, 2018

## Abstract

We develop the idea proposed by Barge & Sommeria (1995) and Tanga *et al.* (1996) that large-scale vortices present in the solar nebula can concentrate dust particles and facilitate the formation of planetesimals and planets. We introduce an exact vortex solution of the incompressible 2D Euler equation and study the motion of dust particles in that vortex. In particular, we derive analytical expressions for the capture time and the mass capture rate as a function of the friction parameter. Then, we study how small-scale turbulent fluctuations affect the motion of the particles in the vortex and determine their rate of escape by solving a problem of quantum mechanics. We apply these results to the solar nebula and find that the capture is optimum near Jupiter's orbit (as noticed already by Barge & Sommeria 1995) but also in the Earth region. This second optimum corresponds to the transition between the Epstein and the Stokes regime which takes place, for relevant particles, at the separation between telluric and giant planets (i.e near the asteroid belt). At these locations, the particles are efficiently captured and concentrated by the vortices and can undergo gravitational collapse to form the planetesimals.

## 1 Introduction

Many astrophysical objects, ranging from young stars to massive black holes, are surrounded by widespread gaseous disks. The existence of a primordial disk around the sun was conjectured by Kant (1755) and Laplace (1796) in the 18<sup>th</sup> century to explain the quasi-circular, coplanar and prograd motion of the planets in the solar system. Such protoplanetary disks have recently been observed with the Hubble Space Telescope in the Orion nebula around stars less than one million years old. These gaseous disks can be considered as a by-product of the star formation: after the gravitational collapse of a molecular cloud, about 99% of the initial angular momentum is spread in an extended disk, while 99% of the mass forms the star, whose internal structure is hardly affected by rotation.

Whenever it has been possible to observe rotating, turbulent fluids with good resolution, it has been seen that individual, intense vortices form (Bengston & Lighthill 1982; Hopfinger *et al.* 1983; Dowling and Spiegel 1990). One of the most striking example is Jupiter's Great Red Spot, a huge vortex persisting for more than three centuries in the

upper atmosphere of the planet. These coherent vortices are well reproduced in numerical simulations (McWilliams 1990, Marcus 1990) and laboratory experiments (Van Heist & Flor 1989, Sommeria, Meyers & Swinney 1988) of two-dimensional turbulence and their organization can be explained in terms of statistical mechanics (Miller 1990, Robert & Sommeria 1991, Sommeria *et al.* 1991, Chavanis & Sommeria 1998)<sup>1</sup>. It seems therefore natural to expect their presence in accretion disks also (Dowling & Spiegel 1990, Abramowicz *et al.* 1992, Adams & Watkins 1995).

However, accretion disks are exceptional among rotating turbulent objects in the strong shears that these bodies are believed to possess and this shear might lead to rapid destruction of any structures that tend to form. This objection has been overruled by the numerical simulations of a two-dimensional flow in an external Keplerian shear by Bracco *et al.* (1998,1999) for an incompressible flow and Godon & Livio (1999a,b,c) for a compressible flow. Although cyclonic fluctuations are rapidly elongated and destroyed by the shear, anticyclonic vortices form and persist for a long time before being ultimately dissipated by viscosity. Naturally, this does not prove that coherent structures must form on disks, but this strengthens the argument that disks are likely to follow the norm of rotating, turbulent bodies. Other numerical results (Hunter & Horak 1983) and experimental work (Nezlin & Snezhkin 1993) comfort this point.

Coherent vortices in circumstellar disks can play an important role in the transport of dust particles and in the process of planet formation. Planets are thought to be formed from the dust grains embedded in the disk after a three-stage process: (i) in a first stage, microscopic particles suspended in the gas stick together on contact due to electrostatic or surface forces. When they reach sufficient sizes, they begin to sediment in the mid-plane of the disk due to the combined effect of the gravity and the friction with the gas. When settling dominates, a particle can grow by sweeping up smaller ones (Safronov 1969) and may easily reach sizes of several centimeters in a few thousand orbital periods (Weidenschilling & Cuzzi 1993). Bigger aggregates ( $> 100cm$ ) are more difficult to form on relevant time scales because of collisional fragmentation (ii) When the layer of sedimented particles is sufficiently dense, the gravitational instability is triggered and the layer crumbles into numerous kilometer-sized bodies, the so-called “planetesimals” (Safronov 1969, Goldreich & Ward 1973). (iii) The subsequent evolution is marked by planet’s growth due to the accumulation of planetesimals in successive collisions. This stage is well reproduced by dynamical models (Safronov 1969, Barge & Pellat 1991, 1993). When the solid core becomes sufficiently massive, it can accrete the surrounding gas and a giant planet, like Jupiter, is formed.

However, the above scenario faces two major problems. Recent studies have shown that circumstellar disks are relatively turbulent and that small-scale turbulence strongly reduces the sedimentation of the dust particles in the ecliptic plane (Weidenschilling 1980, Cuzzi *et al.* 1993, Dubrulle *et al.* 1995). For particles of relevant size, the density of the dust layer is not sufficient to overcome the threshold imposed by Jeans instability criterion. Therefore,

---

<sup>1</sup>It can be noted that the statistical mechanics of two-dimensional turbulence is very similar to the theory of “violent relaxation” (Lynden-Bell 1967) by which galaxies achieve an equilibrium state. It is fascinating to realize that despite their very different physical nature, two-dimensional vortices and stellar systems share some common features. This analogy is developed in detail in Chavanis *et al.* (1996) and Chavanis (1996,1998a,1999).

the formation of the planetesimals, i.e the passage from *cm*-sized to *km*-sized particles, is not clearly understood. In addition, it seems difficult, with the above model, to build up sufficiently massive cores in less than one million years before the gas has been swept away by the solar wind during the T-tauri phase (Safronov 1969, Wetherill 1988).

Both difficulties are ruled out if we allow for the presence of vortices in the disk. Their existence was first proposed by Von Weizsäcker (1944) to explain the regularity of the planet distribution in the solar system: the famous Titius-Bode law <sup>2</sup>. This idea has been reintroduced recently by Barge & Sommeria (1995) and Tanga *et al.* (1996) who demonstrated that anticyclonic vortices in a rotating disk are able to capture and concentrate dust particles. The capture is made possible by the action of the Coriolis force which pushes the particles inward. These results are supported by a dynamical model which integrates the motion of the particles in the velocity field produced by a full Navier-Stokes simulation of the gas component (Bracco *et al.* 1999, Godon & Livio 1999c). It is found that the particles are very efficiently captured and concentrated by the vortices. This is interesting because, without a confining mechanism, *cm*-sized bodies would rapidly fall onto the sun due to the inward drift associated with the velocity difference between gas and particles. Inside the vortices, the density of the dust cloud is increased by a large factor which is sufficient to trigger *locally* the gravitational instability and facilitate the formation of the planetesimals or the cores of giant planets. This trapping mechanism is quite rapid (a few rotations) and can reduce substantially the time scale of planet formation.

In this paper, we present a simple analytical model for the capture of dust particles by coherent vortices in a rotating disk. This model is directly inspired by the numerical studies of Barge & Sommeria (1995) and Tanga *et al.* (1996) and their main results are recovered and confirmed. One interest of our approach is to provide analytical results (leading to quantitative predictions) and to isolate relevant parameters which prove to be particularly important in the problem. In section 2, we introduce an exact solution of the incompressible 2D Euler equation appropriate to our study. This is an elliptic vortex with uniform vorticity matching continuously with the azimuthal Keplerian flow at large distances. We consider deterministic trajectories of dust particles in that vortex and derive analytical expressions for the capture time and the mass capture rate as a function of the friction parameter. In section 3, we investigate the effect of small-scale turbulence on the motion of the particles. Their trajectories become stochastic and their motion must be described in terms of diffusion equations. We estimate the diffusion coefficient and determine the typical length on which the particles are concentrated in the vortices. In section 4, we evaluate the rate of particles which diffuse away from the vortices due to turbulent fluctuations. An explicit expression for the “rate of escape” is obtained by solving a problem of quantum mechanics, namely a two-dimensional oscillator in a box. In appendix A, we give some details about the construction of the vortex solution and in appendix B, we extend Toomre instability criterion (Toomre, 1964) to the case of a *turbulent* rotating disk.

In parallel, we apply these theoretical results to the solar nebula and make speculations about its actual structure. For relevant particles going from 10 cm to 100 cm in size, we

---

<sup>2</sup>An account of Von Weizsäcker’s theory can be found in Chandrasekhar (1946). Note that the idea of vortices in the solar system goes back to Descartes (1643)

remark that the transition between the Stokes and the Epstein regimes (at which the gas drag law changes) corresponds precisely to the transition between telluric (inner) and giant (outer) planets. Moreover, in each zone there is a preferred location where the capture of dust by vortices is *optimal*. For particles of density  $\rho_s \sim 2 \text{ g/cm}^3$  and size  $\sim 30 \text{ cm}$  (a typical prediction of grain growth models), this is near the Earth orbit in the Stokes (inner) zone and between Jupiter and Saturn in the Epstein (outer) zone. For a broader class of parameters, the preferred locations cover the whole region of telluric and giant planets with a depletion near the asteroid belt. Inside the vortices, the surface density of the dust particles is increased by a factor 100 or more sufficient to trigger *locally* the gravitational instability. More precisely, we study how the surface density enhancement depends on the size of the particles. We show that particles must have reached at least centimetric sizes to collapse and form the planetesimals. Smaller particles diffuse away from the vortices on account of turbulent fluctuations and are not sufficiently concentrated. This implies that sticking processes are necessary to produce large particles. These results rehabilitate the Safronov-Goldreich-Ward scenario in localized regions of the disk (i.e, inside the vortices) and for sufficiently large (decimetric) particles. Preliminary results of this work were presented in Chavanis (1998b).

## 2 Deterministic motion of a particle in a vortex

### 2.1 The solar nebula model

We assume that the solar nebula is disk-shaped and is in hydrostatic equilibrium in the vertical direction. If the mass of the disk is much less than the solar mass ( $< 0.1M$ ), then its self-gravity can be neglected compared with the sun's attraction. In that case, the disk has approximately Keplerian rotation

$$\Omega(r) = \left( \frac{GM}{r^3} \right)^{1/2} \quad (1)$$

where  $r$  is the distance from the sun and  $G = 6.672 \cdot 10^{-8} \text{ cm}^3/(\text{g}\cdot\text{s}^2)$  the constant of gravity. For thin disks, the vertical component of the solar gravity is:

$$g_z \simeq -\frac{GM}{r^2} \times \frac{z}{r} = -\Omega^2 z \quad (2)$$

The condition of hydrostatic equilibrium implies that the vertical pressure gradient is precisely balanced by  $g_z$ , i.e:

$$\frac{\partial p}{\partial z} = -\rho_g \Omega^2 z \quad (3)$$

If the local temperature  $T = \frac{m}{k} \frac{p}{\rho_g}$  is independent of  $z$ , then the vertical density profile of the gas is

$$\rho_g = \rho_0 e^{-z^2/H^2} \quad (4)$$

The half-thickness (or scale height) of the disk is given by

$$H = c_s/\Omega \quad (5)$$

where  $c_s \sim \sqrt{\frac{kT}{m}}$  is the sound speed. Other plausible temperature profiles, e.g. adiabatic gradient in the  $z$  direction yield similar results.

We assume also that the gas is turbulent. Turbulence is necessary to explain the dynamical evolution of the protoplanetary disk and its cooling consistent with cosmochemical data (Dubrulle 1993). However, its origin is not well understood and remains controversial. Various mechanisms for inducing global nebula turbulence have been proposed. Lin & Papaloizou (1980) and Cabot *et al.* (1987a,b) suggested that thermal convection drives nebula turbulence. However, the applicability of their results depends on the presence of abundant micron-sized dust to provide substantial thermal opacity; thus, they are questionable when significant particle growth has already occurred and the thermal opacity has decreased. Dubrulle (1992,1993) suggested that the Keplerian shear is the main engine of the turbulence. This was already pointed out by Von Weizsäcker and further discussed by Chandrasekhar (1949) in view of the very small viscosity of the disk: “The successive rings of gas in the medium will have motions relative to one another, and turbulence will ensue”. This apparently obvious claim is actually far from straightforward to support because the Keplerian shear is stable with respect to linear, infinitesimal, perturbations which are usually relied upon to induce turbulence. However, Dubrulle & Knobloch (1992) point out that it might be unstable to nonlinear finite amplitude perturbations, a property shared by most of the shear flows commonly met in engineering or laboratory experiments. The simplest example is the plane Couette flow, a plane parallel stream of constant shear. This analogy is contested by Balbus *et al.* (1996) who didn’t evidence nonlinear instabilities in Keplerian disks at the respectable Reynolds numbers they achieved numerically<sup>3</sup>. These authors have suggested, in contrast, that turbulence in Keplerian disks could be produced by a powerful MHD instability (Balbus & Hawley 1991). The numerical simulations of Bracco *et al.* (1998) suggest that MHD turbulence can form magnetized vortices able to capture charged particles. However, in the case of the disk that is supposed to have spawned the solar system, it is thought that the matter was too cool to be ionized. The recourse to magnetic effects to render the disk turbulent is therefore suspect and the problem of whether Keplerian disks are turbulent or not remains open. Recently, Lovelace *et al.* (1999) discovered a linear nonaxisymmetric instability in a thin Keplerian disk which can lead to the formation of Rossby vortices. This may open new perspectives for hydrodynamical turbulence in accretion disks.

In any case, the solar nebula must have been turbulent at least during its formation from the collapsing protostar, because of velocity discontinuities as the infalling matter struck the disk. The infall probably did not stop suddenly but decayed over some interval. Therefore, the initial conditions in the disk were turbulent and this is sufficient to form vortices that survive for many rotation periods of the disk (Bracco *et al.* 1998,1999; Godon & Livio 1999a,b,c). The appearance of large-scale coherent vortices in rotating flows is due to the presence of the Coriolis force and the bimodal nature of turbulence (Dubrulle & Valdetaro 1992). At small scales, the influence of the rotation is negligible and the turbulence is homogeneous and isotropic. Energy cascades towards smaller and smaller scales up to the dissipation length. Turbulent diffusion is important and can accelerate

---

<sup>3</sup>See also the 2D simulations by Godon & Livio (1999a) starting from finite perturbations who showed that turbulence is not self-sustained.

the mixing of dust particles. At larger scales, the Coriolis force becomes dominant and the gas dynamics is quasi two-dimensional. On these scales, the energy transfers are inhibited or even reversed; this is a manifestation of the celebrated “inverse cascade” process (see, e.g. Kraichnan & Montgomery 1980) in two-dimensional turbulence. There is therefore the possibility of formation and maintenance of coherent vortices (Mc Williams 1990). These vortices can form either by a large-scale instability (Frisch *et al.* 1987, Dubrulle & Frisch 1991, Kitchatinov *et al.* 1994) or by the successive mergings of like-sign vortices, as observed in the simulations of Bracco *et al.* (1998,1999) and Godon & Livio (1999a,b,c). Due to the strong Keplerian shear, only anticyclonic vortices can survive this process. Initially, the vortices have size  $R \ll H$  and typical vorticity  $\Omega$ . Their velocity  $v \sim \Omega R$  is less than the sound speed  $c_s = \Omega H$  and the flow can be considered as incompressible. The merging ends up when the Mach number  $Ma = \frac{v}{c_s}$  reaches unity, i.e  $R \sim H$ . Bigger vortices radiate density waves and do not maintain (see Barge & Sommeria 1995).

We expect therefore that, after some evolution, the disk be filled with anticyclonic vortices of typical size  $H$ , the disk thickness. Vortices are expected to form throughout the nebula and there is no reason, a priori, to believe that certain regions of the disk should be excluded. However, two vortices at comparable distance from the sun will approach each other (due to differential rotation) and finally merge. Therefore, we do not expect more than one (or a few) vortices at each radial distance. On the other hand, two successive vortices should be separated by a distance comparable to their size  $R$ . Since  $R \sim H$  and  $H$  scales like a power law of the distance to the sun ( $r^{5/4}$  in the standard model considered below), the distribution of vortices should be consistent with an approximate geometric progression of the planetary positions (Barge & Sommeria 1995). As elucidated by Graner & Dubrulle (1994), the Titius-Bode law reflects more the general properties of scale invariance in the solar nebula than any particular physical process.

## 2.2 The vortex model

We consider the motion of a dust particle in a vortex located at a distance  $r_0$  from the sun. For convenience, we work in a frame of reference rotating with constant angular velocity  $\Omega \equiv \Omega(r_0)$  and we denote by  $\mathbf{u}(\mathbf{r}, t)$  the velocity field of the gas in that frame. The dust particle is subjected to the attraction of the sun  $-\frac{GM}{r^3}\mathbf{r}$  and to a friction with the gas that we write  $-\xi(\mathbf{v} - \mathbf{u}(\mathbf{r}, t))$  where  $\mathbf{v} = \frac{d\mathbf{r}}{dt}$  is the particle velocity. We shall come back to this expression and to the value of the friction coefficient  $\xi$  in section 2.5. Since we work in a rotating frame, apparent forces arise in the system. These are the Coriolis force  $-2\boldsymbol{\Omega} \wedge \mathbf{v}$  and the centrifugal force  $\Omega^2\mathbf{r}$ . All things considered, the particle equation writes:

$$\frac{d^2\mathbf{r}}{dt^2} = -\xi\left(\frac{d\mathbf{r}}{dt} - \mathbf{u}(\mathbf{r}, t)\right) - 2\boldsymbol{\Omega} \wedge \frac{d\mathbf{r}}{dt} + \left(\Omega^2 - \frac{GM}{r^3}\right)\mathbf{r} \quad (6)$$

This is an ordinary second order differential equation coupled to the gas motion. The case of a time dependant velocity field  $\mathbf{u}(\mathbf{r}, t)$  produced by the Navier-Stokes simulation of a random initial vorticity field superposed on the Keplerian rotation has been investigated by Bracco *et al.* (1999) and Godon & Livio (1999c) who observed the capture of the dust particles by anticyclonic vortices. The case of a static velocity field  $\mathbf{u}(\mathbf{r})$  was first considered by Barge & Sommeria (1995) and Tanga *et al.* (1996) with different vortex profiles. Barge

& Sommeria (1995) assume that the velocity field inside the vortex is made of concentric epicycles while it matches continuously the Keplerian flow at large distances. This epicyclic model is motivated by the underlying idea that the particles, when sufficiently concentrated, will retroact on the vortex and will force the gas to follow their natural motion. Tanga *et al.* (1996) consider a more complex streamfunction describing an ensemble of small vortices corresponding to Rossby waves corotating with the flow. This velocity field is obtained as a self-similar solution of the linearized equations of motion governing the large-scale dynamics of a turbulent nebula. These two models lead to qualitatively similar results indicating that dust particles are efficiently trapped into coherent anticyclonic vortices. However, the models differ in the details: in Tanga *et al.* (1996), the particles sink to the center of the vortices with no limit while in Barge & Sommeria (1995), the spiralling motion ends up on an epicycle. In that case, the friction force cancels out and the epicyclic motion is an exact solution of the particle equation (6).

We must note, however, that the vortex constructed by Barge & Sommeria (1995) is relatively *ad hoc* and does not satisfy the fluid equations rigorously. In this article, we introduce an exact vortex solution of the incompressible 2D Euler equation and study analytically the motion of dust particles in that vortex. Since the vortices of the solar nebula are small compared with the radial distance  $r_0$  (we have typically  $R/r_0 \sim 0.04$ , see formula (44)) the last term in equation (6) can be expanded to first order in the displacement  $\mathbf{r} - \mathbf{r}_0$ . This is the so-called “epicyclic approximation”. Introducing a set of cartesian coordinates  $(x, y)$  centered on the vortex and such that the  $y$ -axis points in the direction opposite to the sun, the particle equation (6) reduces to:

$$\frac{d^2x}{dt^2} = -\xi \left( \frac{dx}{dt} - u_x \right) + 2\Omega \frac{dy}{dt} \quad (7)$$

$$\frac{d^2y}{dt^2} = -\xi \left( \frac{dy}{dt} - u_y \right) - 2\Omega \frac{dx}{dt} + 3\Omega^2 y \quad (8)$$

At sufficiently large distances from the vortex, the velocity field is a simple shear:

$$u_x = \frac{3}{2}\Omega y \quad (9)$$

$$u_y = 0 \quad (10)$$

obtained as a first order expansion of the Keplerian velocity around  $\mathbf{r}_0$ . Its vorticity is  $\omega_K \equiv \partial_x u_y - \partial_y u_x = -\frac{3}{2}\Omega$ .

It remains now to specify the velocity field inside the vortex. We can construct an exact solution of the incompressible 2D Euler equation by taking an elliptic patch of uniform vorticity  $\omega$ . This solution is well-known by model builders (see, e.g, Saffman 1992)<sup>4</sup> but, to our knowledge, it has never been applied in an astrophysical context. Therefore, we give a short description of its construction in Appendix A. In the vortex, the velocity field writes

$$u_x = -\frac{q^2}{1+q^2}\omega y \quad (11)$$

---

<sup>4</sup>This solution was indicated to me by J.Sommeria.

$$u_y = \frac{1}{1+q^2}\omega x \quad (12)$$

where  $q = a/b$  is the aspect ratio of the elliptic patch ( $a, b$  are the semi-axis in the  $x$  and  $y$  directions respectively). Outside the vortex, the velocity field is given by equation (174) of Appendix A. At large distances, we recover the Keplerian shear (9)(10).

The matching conditions between the elliptic vortex and the Keplerian shear require that  $\omega$ ,  $\omega_K$  and  $q$  be related according to (see Appendix A):

$$\frac{\omega_K}{\omega} = \frac{q(q-1)}{1+q^2} \quad (13)$$

The solution (11)(12) is valid for  $q > 1$ , implying  $0 < \omega_K/\omega < 1$ . The vortex is *anticyclonic* ( $\omega < 0$ ) and is oriented with its major axis parallel to the shear streamlines. It can be shown to be stable to infinitesimal two-dimensional disturbances. For  $q \rightarrow 1$  (circular vortices),  $\omega \rightarrow -\infty$  and for  $q \rightarrow \infty$  (infinitely elongated vortices),  $\omega \rightarrow \omega_K$ . Therefore,  $\omega$  is in the range  $]-\infty, -\frac{3}{2}\Omega]$ . In a rotating disk, we expect that  $\omega \sim -2\Omega$ , corresponding to a Rossby number of order 1. This value is achieved by vortices with aspect ratio  $q \simeq 4$ , in good agreement with the model of Tanga *et al.* (1996). The epicyclic vortex considered by Barge & Sommeria (1995) corresponds to  $q = 2$  and  $\omega = -\frac{5}{2}\Omega$ . These values do not satisfy the matching condition (13) with the Keplerian shear so the epicyclic vortex is not an exact solution of the incompressible Euler equation. It may be used, however, as an approximate solution if we take into account a coupling between the particles and the gas in the spirit of a two-fluid model.

### 2.3 The capture time

Before going into mathematical details, we recall the argument of Tanga *et al.* (1996) which shows very simply why particles are trapped by anticyclonic vortices in a rotating disk. Introducing a system of polar coordinates  $(r, \theta)$  whose origin coincides with the vortex center, the radial component of equation (6) reads:

$$\frac{d^2r}{dt^2} = r\left(\frac{d\theta}{dt}\right)^2 + 2\Omega r \frac{d\theta}{dt} - \xi\left(\frac{dr}{dt} - u_r\right) + 3\Omega^2 r \sin^2 \theta \quad (14)$$

where we have used the epicyclic approximation. The first term is a centrifugal force due to the rotation of the vortex (not to be confused with the centrifugal force  $\Omega^2 r$  due to the rotation of the disk) and the second term is the Coriolis force. The drag term in equation (6) forces the particle velocity to approach the fluid velocity, i.e.  $\frac{d\theta}{dt} \sim \omega$ . For cyclonic vortices ( $\omega > 0$ ), both centrifugal and Coriolis forces are positive and push the particles outward. For anticyclonic vortices ( $\omega < 0$ ), the Coriolis force pushes the particles inward and comes in conflict with the centrifugal force which is always directed outward. If the vortex rotates rapidly, the centrifugal force prevails over the Coriolis force and the particle is expelled. In the other case, the Coriolis term dominates and the particle is captured. We conclude that only slowly rotating anticyclonic vortices can capture dust particles. This trapping process is specific to rotating fluids; in ordinary simulations of two-dimensional turbulence (without Coriolis force) the particles never penetrate the vortices. Note that the



epicyclic acceleration (last term in equation (14)) is always directed outward. This term is responsible for a flux of particles toward the sun (if the gravitational force dominates, i.e for  $y < 0$ ) or toward the outer nebula (if the centrifugal force dominates, i.e  $y > 0$ ). However, this flux is quite small and doesn't affect the overall trapping process (see Tanga *et al.* 1996).

We give now a more precise analysis of the trapping process and try to derive an explicit expression for the capture time of the particles as a function of their friction parameter  $\xi$ . To that purpose, we notice that equations (7) (8) with the velocity field (11) (12) form a *linear* system of coupled differential equations. We seek therefore a solution of the form:

$$x = X e^{\lambda t} \quad (15)$$

$$y = Y e^{\lambda t} \quad (16)$$

where  $X, Y$  and  $\lambda$  are complex numbers. Substituting into equations (7) (8), we obtain a linear system of algebraic equations:

$$-\lambda(\lambda + \xi)X + 2\Omega \left( \frac{3}{4} \frac{q}{q-1} \xi + \lambda \right) Y = 0 \quad (17)$$

$$\left( \frac{3\Omega}{2} \frac{1}{q(q-1)} \xi + 2\Omega\lambda \right) X + (\lambda\xi + \lambda^2 - 3\Omega^2) Y = 0 \quad (18)$$

There are nontrivial solutions only if the determinant of this system is zero. We are led therefore to a fourth order polynomial equation in  $\lambda$ :

$$\begin{aligned} \lambda^4 + 2\xi\lambda^3 + (\xi^2 + \Omega^2)\lambda^2 + 3\frac{1+q}{q(q-1)}\xi\Omega^2\lambda \\ + \frac{9}{4}\xi^2\Omega^2\frac{1}{(q-1)^2} = 0 \end{aligned} \quad (19)$$

By definition, we will say that a particle is *light* or *heavy* whether  $\xi > \Omega$  or  $\xi < \Omega$  respectively. This terminology will take more sense in the sequel (see in particular section 2.5). We now consider the asymptotic limits  $\xi \rightarrow \infty$  and  $\xi \rightarrow 0$  of equation (19).

For  $\xi \rightarrow \infty$  (light particles), the four roots of equation (19) are

$$\lambda = -\xi \quad (\text{double root}) \quad (20)$$

$$\lambda = \pm \frac{3\Omega}{2(q-1)}i - \frac{3\Omega^2(q-2)(2q+1)}{4\xi q(q-1)^2} \quad (21)$$

The first solution is rapidly damped and will not be considered anymore. The second solution describes the rotation of the dust particles in the vortex:

$$x = A \cos \left[ -\frac{3\Omega}{2(q-1)}t \right] e^{-t/t_{capt}} \quad (22)$$

$$y = \frac{A}{q} \sin \left[ -\frac{3\Omega}{2(q-1)}t \right] e^{-t/t_{capt}} \quad (23)$$

The particles follow ellipses of aspect ratio  $q$  and move with angular velocity  $-\frac{3\Omega}{2(q-1)}$ . In fact, for  $\xi \rightarrow \infty$ , the drag term in equation (6) implies  $\frac{d\mathbf{r}}{dt} \simeq \mathbf{u}$  so, in a first approximation, the particles just follow the vortex streamlines (their angular velocity coincides with the angular velocity of the fluid particles, see Appendix A). In addition, they experience a *drift* toward the center due to the combined effect of the friction and the Coriolis force. They reach the vortex center in a typical time:

$$t_{capt} = \frac{4\xi}{3\Omega^2} \frac{q(q-1)^2}{(q-2)(2q+1)} \quad (24)$$

defined as the *capture time*. Note that for light particles,  $t_{capt}$  increases *linearly* with  $\xi$ .

For  $\xi \rightarrow 0$  (heavy particles), the four roots of equation (19) are:

$$\lambda = -\frac{3}{2} \frac{1+q \pm \sqrt{1+2q}}{q(q-1)} \xi \quad (25)$$

$$\lambda = \pm \Omega i - \frac{(q-3)(2q+1)}{2q(q-1)} \xi \quad (26)$$

The second solution describes again a damped rotation of the particles but with a different trajectory:

$$x = A \cos(-\Omega t) e^{-t/t_{capt}} \quad (27)$$

$$y = \frac{A}{2} \sin(-\Omega t) e^{-t/t_{capt}} \quad (28)$$

The particles follow ellipses with aspect ratio 2 and move with angular velocity  $-\Omega$ . This is natural since heavy particles have the tendency to decouple from the gas and reach a pure epicyclic motion. However, due to a slight friction, they sink progressively in the vortex with a characteristic time

$$t_{capt} = \frac{2q(q-1)}{(q-3)(2q+1)} \frac{1}{\xi} \quad (29)$$

For heavy particles, the capture time increases like  $\xi^{-1}$ . Very heavy particles can even leave the vortex. Formally, this possibility is taken into account in the first solution (25) which corresponds to open trajectories. The motion of heavy particles is therefore more complicated and demands a numerical integration of the particle equation inside and outside the vortex. This study will not be undertaken in that paper. We shall only consider the case of closed trajectories described by equations (27)(28).

For intermediate values of  $\xi$ , the capture time and the angular velocity of the particles are plotted on figures 1 and 2 (for the particular value  $q = 4$ ). We see that  $t_{capt}$  presents an optimum at  $\xi = \xi_{opt}$ . Moreover, the asymptotic expressions (24) and (29) agree reasonably well with the exact solution for all the values of the friction parameter. Therefore, considering the intersection of the asymptotes, we find that the capture time is minimum for

$$\xi_{opt} \simeq \left[ \frac{3(q-2)}{2(q-1)(q-3)} \right]^{1/2} \Omega \quad (30)$$

and we have:

$$t_{capt}^{min} \simeq \left[ \frac{8(q-1)^3 q^2}{3(q-3)(2q+1)^2(q-2)} \right]^{1/2} \frac{1}{\Omega} \quad (31)$$

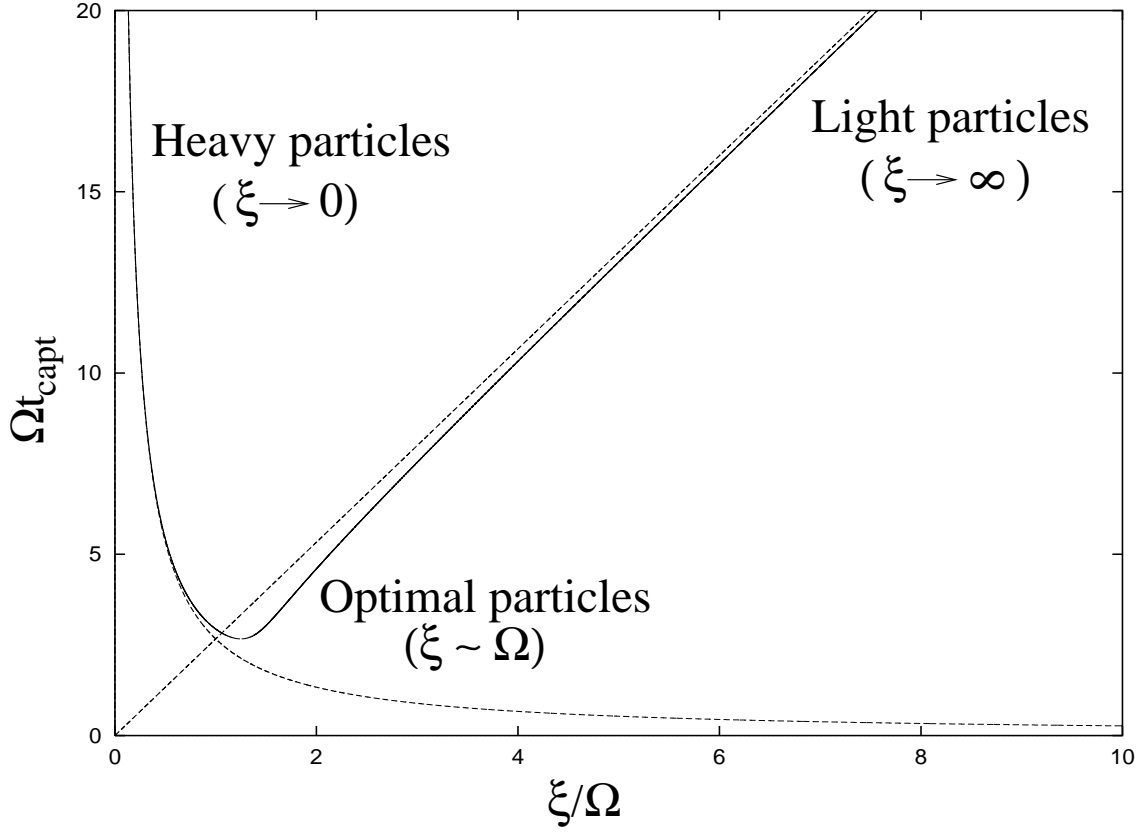


Figure 1: Plot of  $t_{capt}$  vs  $\xi$  for vortices with aspect ratio  $q = 4$ . The dash lines correspond to formulae (24) and (29) valid for light ( $\xi \rightarrow \infty$ ) and heavy ( $\xi \rightarrow 0$ ) particles.

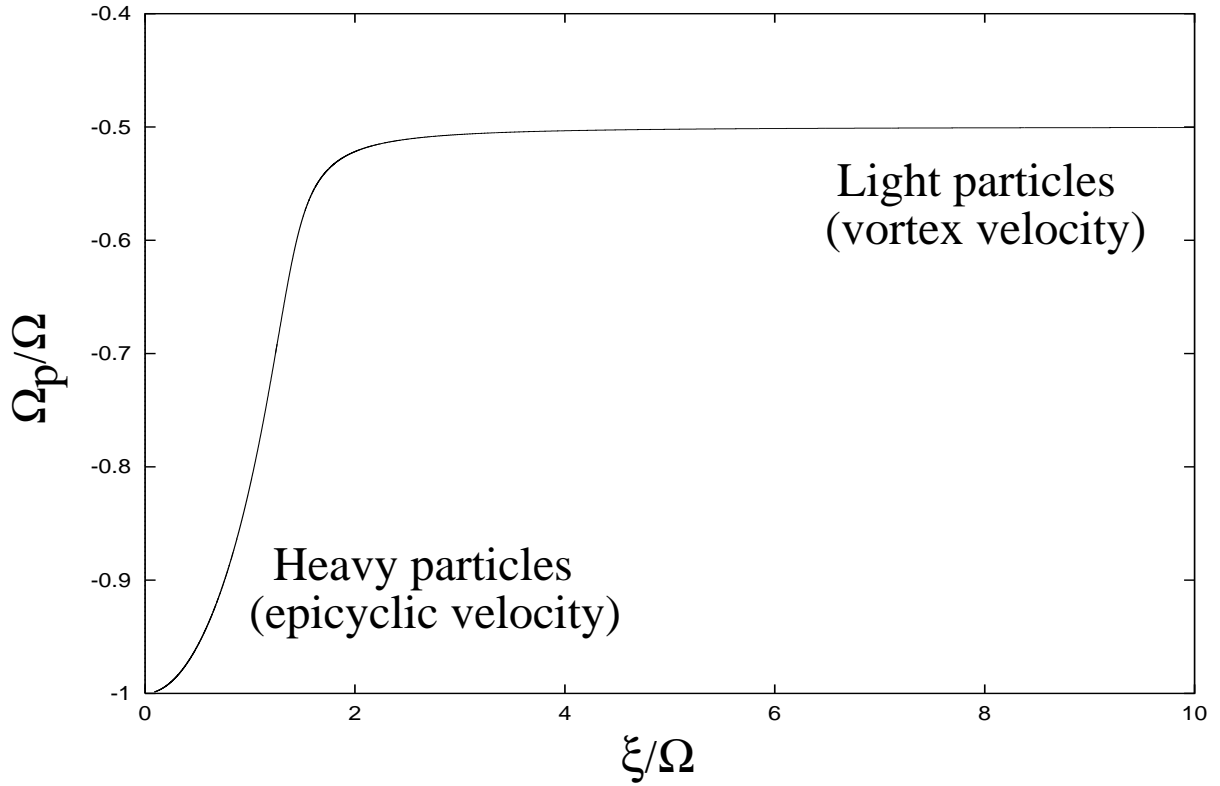


Figure 2: Plot of  $\Omega_p$  (angular velocity of the particles) vs  $\xi$  for vortices with aspect ratio  $q = 4$ . Light particles ( $\xi \rightarrow \infty$ ) move with the vortex velocity  $-\frac{3\Omega}{2(q-1)}$  and heavy particles ( $\xi \rightarrow 0$ ) with the epicyclic velocity  $-\Omega$ .

According to equations (24) and (29), the condition for particle trapping ( $t_{capt} > 0$ ) requires that  $q > 3$ . This implies that the vorticity must be in the range [see equation (13)]:

$$-\frac{5}{2}\Omega < \omega < -\frac{3}{2}\Omega \quad (32)$$

Particles are ejected from rapidly rotating anticyclones in agreement with the qualitative discussion of Tanga *et al.* (1996) recalled at the beginning of this section. In the following, we shall specialize on the value of  $q$  which minimizes the capture time  $t_{capt}^{min}$ . We find  $q \simeq 4$ . As noted already, this value corresponds to  $\omega \simeq -2\Omega$ , i.e a Rossby number of order 1. For these vortices, the optimal friction parameter is  $\xi_{opt} = \Omega$  and the corresponding capture time  $t_{capt}^{min} = \frac{8}{3\Omega}$  is of the order of one rotation period. For  $\xi > \Omega$ , we have

$$t_{capt} \simeq \frac{8\xi}{3\Omega^2} \quad (\text{light particles}) \quad (33)$$

and for  $\xi < \Omega$

$$t_{capt} \simeq \frac{8}{3\xi} \quad (\text{heavy particles}) \quad (34)$$

Light particles move with angular velocity  $-\frac{\Omega}{2}$  (the vortex velocity) and heavy particles move with angular velocity  $-\Omega$  (the epicyclic velocity). These results should be compared with the settling time of the dust particles in the equatorial plane (see, e.g, Nakagawa *et al.* 1986). Light particles are settled exponentially with a characteristic time  $\xi/\Omega^2$  comparable with equation (33). On the other hand, heavy particles undergo overdamped oscillations around the midplane with a period of the order of  $\Omega^{-1}$  and a settling time  $2/\xi$  similar to expression (34). We shall come back on the analogy between the vortex trapping and the dust settling in section 3.1.

The models of Barge & Sommeria (1995) and Tanga *et al.* (1996) lead to qualitatively similar results. In the model of Tanga *et al.* (1995), the particles sink to the center of the vortex on a typical time  $t_{capt}(\xi)$  which also presents a minimum when  $\xi$  is of order  $\Omega$ . Moreover, for light particles,  $t_{capt}$  increases linearly with  $\xi$  like in equation (33). The model of Barge & Sommeria (1995) is physically different since the particles do not really reach the vortex center but end up on an epicycle after a time  $\sim 1/\xi$ . However, the general tendency is the same. Light particles ( $\xi \gg \Omega$ ) mainly follow the streamlines of the gas and stop on epicycles close to the vortex edge (like in case (a) of their figure 1). Optimal particles with friction parameter  $\xi \sim \Omega$  reach deeper epicycles, almost at the center of the vortex (case (b)). Heavy particles ( $\xi \ll \Omega$ ) take a long time to connect an epicycle and can even escape from the vortex since their motion is nearly unaffected by the friction drag. This is also a possibility in our model and in Tanga *et al.* (1996). Therefore, the three vortex models give relatively similar results even if their physical contents are different. The recent numerical simulations of Godon & Livio (1999c) for a compressible flow also show a capture optimum when the drag parameter is of the order of the orbital frequency.

## 2.4 The mass capture rate

In addition to the capture time, an important aspect of the problem concerns the mass capture rate (Barge & Sommeria 1995). This quantity can be estimated as follows. First,

we have to determine the capture cross section of the vortex as a function of the friction parameter  $\xi$ . Without the effect of the drift, a particle with impact parameter  $\eta$  would cross the vortex in a typical time  $t_{cross} \sim R/u_K$ , where  $u_K = \frac{3}{2}\Omega\eta$  is the Keplerian velocity. The particle will be captured by the vortex if, during that time, the deflection due to the drift is precisely of order  $\eta$ . Light particles ( $\xi \rightarrow \infty$ ) follow the edge of the vortex and, for them,  $v_{drift} \sim R/t_{capt}$ . On the other hand, heavy particles ( $\xi \rightarrow 0$ ) keep their rectilinear motion and enter directly the vortex so that, for them,  $v_{drift} \sim \eta/t_{capt}$ . The critical parameter  $\eta_c$  is given by the condition  $t_{cross} \times v_{drift} \sim \eta_c$ . Moreover, for optimal particles with  $\xi \sim \Omega$ , we expect that  $\eta_c \sim R$ . Regrouping all these results, we obtain

$$f(\xi) = \frac{\eta_c}{R} \simeq \left(\frac{\Omega}{\xi}\right)^{1/2} \quad (\text{light particles}) \quad (35)$$

$$f(\xi) = \frac{\eta_c}{R} \simeq \frac{\xi}{\Omega} \quad (\text{heavy particles}) \quad (36)$$

These results agree with the asymptotic behaviour of the function  $f(\xi)$  determined numerically by Barge & Sommeria (1995) in their model.

The mass capture rate can be estimated by assuming that the particles are carried to the vortex by the Keplerian shear  $u_K = \frac{3}{2}\Omega y$ , and that they are continuously renewed by the inward drift (directed towards the sun) associated with the velocity difference  $\Delta V$  between gas and particles (Barge & Sommeria 1995). Another alternative, consistent with the simulations of Bracco *et al.* (1999), is that the particles are already concentrated by the turbulent fluctuations that accompany vortex formation in the early stages of the protoplanetary nebula. It is likely that both mechanisms come into play in the capture process. Considering the first possibility, which can be studied analytically, we have (Barge & Sommeria 1995):

$$\frac{dM}{dt} = 2 \int_0^{\eta_c} \sigma_d u_K dy = \frac{3}{2} \sigma_d \Omega R^2 f^2(\xi) \quad (37)$$

where  $\sigma_d$  is the surface density of the dust particles outside the vortex. The total mass collected by the vortex during its lifetime is

$$M_{life} = \frac{3}{2} (\Omega t_{life}) \sigma_d R^2 f^2(\xi) \quad (38)$$

The mass capture rate is proportional to the effective surface  $\sim f^2(\xi)R^2$  of the vortex. As first emphasized by Barge & Sommeria (1995), it is maximum for particles with  $\xi \sim \Omega$ .

In conclusion, various vortex models and different physical arguments show that the capture is *optimal* for particles whose friction parameter is close to the disk rotation. We shall now consider the implications of this result on the structure of the solar nebula.

## 2.5 Application to the solar nebula

We shall assume that the solid particles are spherical, of radius  $a$  and density  $\rho_s$ . The value of the friction parameter  $\xi$  depends whether the size of the particles is larger or smaller than the mean free path  $\lambda$  in the gas (see, e.g. Weidenschilling 1977). When  $a < \frac{9}{4}\lambda$ , we are in the Epstein regime and:

$$\xi = \frac{\Omega \sigma_g}{2\rho_s a} \quad (39)$$

where  $\sigma_g$  is the gas surface density.

When  $a > \frac{9}{4}\lambda$ , the situation is more complicated because, in general, the friction parameter depends on the velocity difference  $|\mathbf{v} - \mathbf{u}|$  between the particles and the gas. There is, however, a regime where  $\xi$  is independent of the particle relative velocity. This is the Stokes regime in which:

$$\xi = \frac{9\sigma_g\Omega\lambda}{8a^2\rho_s} \quad (40)$$

This regime is valid when the particle Reynolds number  $R_p = \frac{2a}{\nu_g}|\mathbf{v} - \mathbf{u}|$ , where  $\nu_g = \frac{1}{2}c_s\lambda$  is the kinematic viscosity of the gas, is smaller than 1. This is the case for light particles which move typically with the gas velocity  $\mathbf{v} \simeq \mathbf{u}$ . For heavy particles on the contrary, we have  $R_p > 1$  and, rigorously speaking, the friction parameter depends on the relative velocity. The use of a more exact expression for  $\xi$  would require a numerical integration of the particle trajectory but the results shouldn't dramatically differ from those obtained with expression (40). Since we are mainly interested by orders of magnitude, we will use expression (40) for all particle sizes (with  $a > \frac{9}{4}\lambda$ ), but keep in mind this uncertainty for large particles.

We shall adopt a standard model of the solar nebula, following Cuzzi *et al.* (1993). It corresponds to a “minimum mass” circumstellar nebula with parameters:

$$\Omega = 2\pi \left( \frac{r}{1\text{A.U.}} \right)^{-3/2} \text{ years}^{-1} \quad (41)$$

$$\sigma_d = 10 \left( \frac{r}{1\text{A.U.}} \right)^{-3/2} \text{ g/cm}^2 \quad (42)$$

$$\sigma_g = 1700 \left( \frac{r}{1\text{A.U.}} \right)^{-3/2} \text{ g/cm}^2 \quad (43)$$

$$H = 0.04 \left( \frac{r}{1\text{A.U.}} \right)^{5/4} \text{ A.U.} \quad (44)$$

$$\lambda = 1 \left( \frac{r}{1\text{A.U.}} \right)^{11/4} \text{ cm} \quad (45)$$

We take 1 year =  $3.15 \cdot 10^7$  s and 1 A.U. =  $1.49 \cdot 10^{13}$  cm.

For a given type of particles, the transition between the Epstein and the Stokes regime is achieved at a specific distance from the sun given by:

$$r_c = \left( \frac{4}{9} \frac{a}{1\text{cm}} \right)^{\frac{4}{11}} \text{ A.U.} \quad (46)$$

We are particularly interested by particles of order 10 cm in size. Indeed, smaller particles can grow by aggregation processes without the aid of vortices. However, when they reach decimetric sizes, collisional fragmentation becomes prohibitive and prevents further evolution (on relevant time scales). It is therefore at this range of sizes that the vortex scenario

should come at work and facilitate the formation of bigger structures, the so-called planetesimals. For particles between 10 and 100 cm in size, we find that the critical radius (46) at which the gas drag law changes lies in the range:

$$1.7A.U < r_c < 3.9A.U \quad (47)$$

that is to say just at the separation between telluric (inner) and giant (outer) planets. This result is relatively robust because it depends only on a small power of the particles size and is independant on their density. We can therefore wonder if there is not a connection between the division of the solar system in two groups of planets (telluric and gaseous) and the two regimes (Stokes and Epstein) of the gas drag law in the primordial nebula. In the following we show how the vortex scenario can give further support to this idea.

Since the friction coefficient of a particle with size  $a$  and density  $\rho_s$  depends on parameters (like  $\sigma_g$ ,  $\lambda$  and  $\Omega$ ) which are functions of the distance  $r$  from the sun, the friction coefficient  $\xi$  is itself a function of  $r$ . Combining equations (39) (40) with equations (41) (43) (45), we obtain:

$$\frac{\xi}{\Omega} = \frac{1913}{a^2 \rho_s} r^{\frac{5}{4}} \quad \text{if } r < r_c \quad (\text{Stokes zone}) \quad (48)$$

$$\frac{\xi}{\Omega} = \frac{850}{a \rho_s} r^{-\frac{3}{2}} \quad \text{if } r > r_c \quad (\text{Epstein zone}) \quad (49)$$

where  $r$  is measured in A.U,  $a$  in cm and  $\rho_s$  in g/cm<sup>3</sup>.

According to the results of section 2.3, the capture time  $\Omega t_{capt}$  (measured in rotation periods) is optimal when  $\xi/\Omega = 1$ . Since  $\xi/\Omega$  is a function of  $r$  with a maximum at  $r_c$ , this criterion determines *two* preferred locations in the disk, one in each zone (see figure 3). In the Stokes (inner) zone, the optimum is at:

$$r_{in} = \left( \frac{a^2 \rho_s}{1913} \right)^{4/5} \quad (50)$$

and in the Epstein (outer) zone, it is at:

$$r_{out} = \left( \frac{850}{a \rho_s} \right)^{2/3} \quad (51)$$

More generally, we can combine equations (33) (34) with equations (48) (49) to express the capture time  $\Omega t_{capt}$  as a function of the distance to the sun (for a given type of particles). We find a W-shaped curve (see figure 4) determined by the power laws:

$$\Omega t_{capt} = \frac{a^2 \rho_s}{717} r^{-5/4} \quad (r < r_{in}) \quad (52)$$

$$\Omega t_{capt} = \frac{5101}{a^2 \rho_s} r^{5/4} \quad (r_{in} < r < r_c) \quad (53)$$

$$\Omega t_{capt} = \frac{2267}{a \rho_s} r^{-3/2} \quad (r_c < r < r_{out}) \quad (54)$$



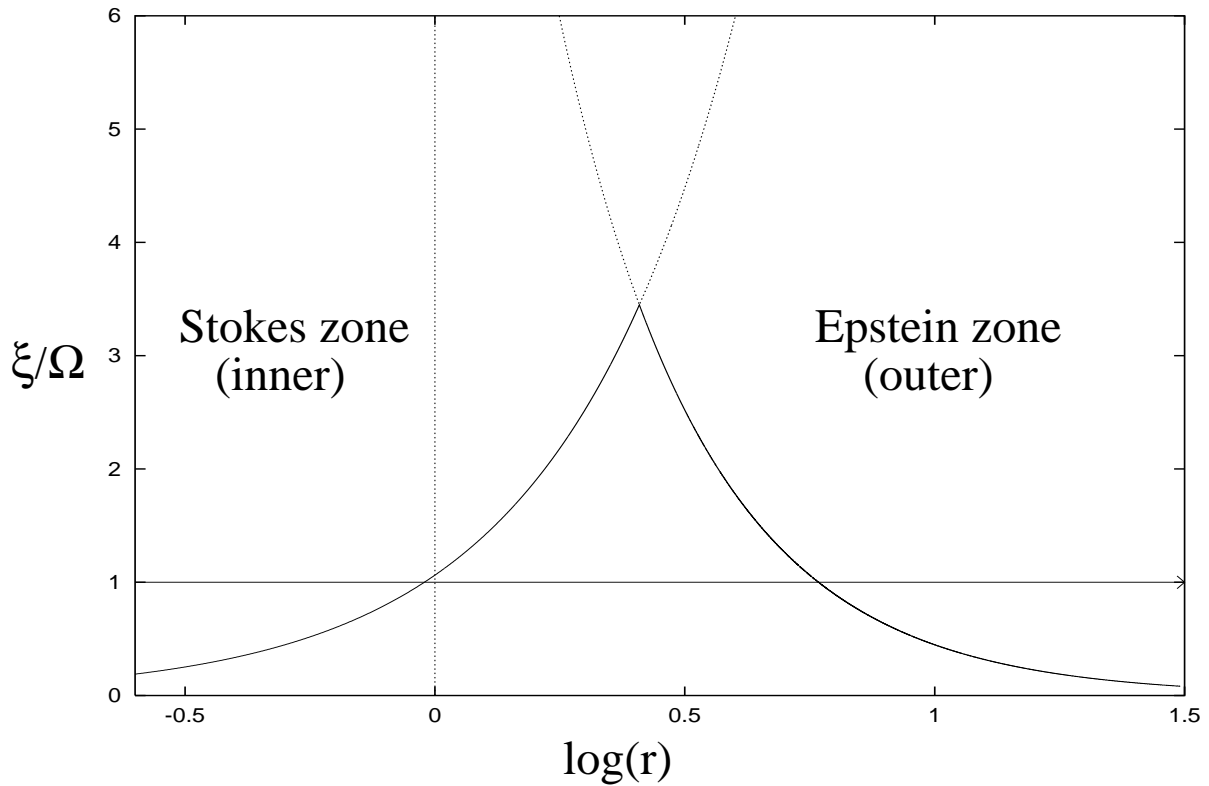


Figure 3: Evolution of the friction parameter  $\xi/\Omega$  as a function of the distance to the sun for a given type of particles (the figure corresponds to particles with size  $a = 30 \text{ cm}$  and bulk density  $\rho_s = 2 \text{ g/cm}^3$ ). The friction parameter is maximum at  $r = r_c$  where the gas drag law passes from the Stokes to the Epstein regime. The condition  $\xi/\Omega = 1$  determines two optimal regions in the disk.

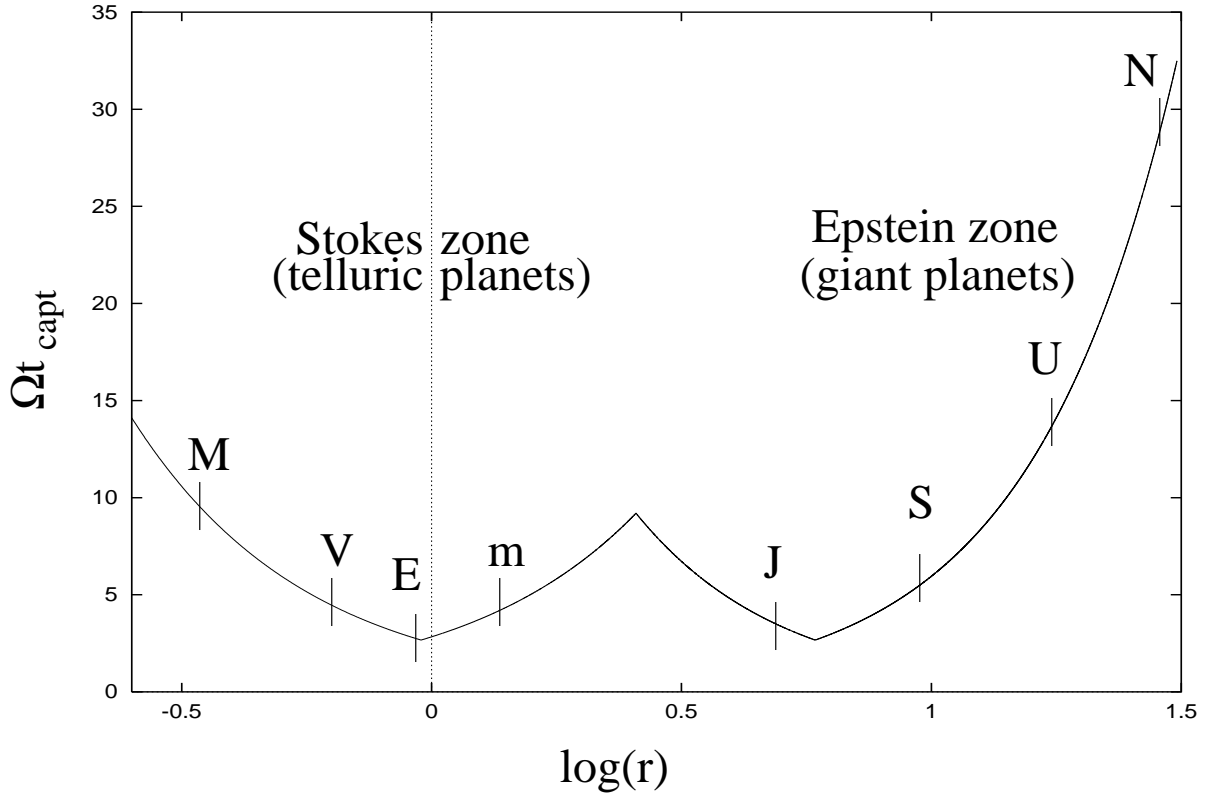


Figure 4: Evolution of the capture time  $\Omega t_{capt}$  as a function of the distance to the sun for a given type of particles ( $a = 30 \text{ cm}$ ,  $\rho_s = 2 \text{ g/cm}^3$ ). We have represented the present position of the planets. The capture time is optimum near the Earth (in the Stokes zone) and between Jupiter and Saturn (in the Epstein zone).

Table 1: Minimum sizes of dust particles (in  $cm$ ) which can trigger the gravitational instability ( $\rho_s = 2g/cm^3$ ).

<i>Planets</i>	$r(A.U)$	$\lambda$	$a_{opt}$	$a_{min}^{conc}$	$a_{min}^{capt}$	$a_{min}$
Telluric planets :						
<i>Mercury</i>	0.387	0.07	17	14	7	3
<i>Venus</i>	0.723	0.4	25	20	11	5
<i>Earth</i>	1	1	31	25	13	6
<i>Mars</i>	1.52	3	40	33	17	8
Asteroid belt :	3	20	61	50	15	3
Giant planets :						
<i>Jupiter</i>	5.20	93	36	23	7	1
<i>Saturn</i>	9.52	492	14	9	3	0.5
<i>Uranus</i>	19.2	3364	5	3	1	0.2
<i>Neptune</i>	30.0	11523	3	2	0.5	0.1

$$\Omega t_{capt} = \frac{a\rho_s}{319}r^{3/2} \quad (r > r_{out}) \quad (55)$$

In order to make a numerical application, we assume that all the particles have the same density  $\rho_s \sim 2g/cm^3$  (the density of a composite rock-ice material) and the same size  $a \sim 30cm$  (a typical prediction of grain growth models). In principle, we should consider a spectrum of sizes and densities but we choose these particular values in order to illustrate at best the predictions of the vortex model. For these values, the optimum in the inner zone is at  $r_{in} \sim 1A.U$ , i.e near the Earth orbit, and the optimum in the outer zone is at  $r_{out} \sim 6A.U$ , i.e between Jupiter and Saturn's orbits. The transition between the Stokes and the Epstein regime occurs at  $r_c \sim 2.7A.U$ , i.e near the asteroid belt.

Alternatively, we can determine, at each heliocentric distance, the size of the particles which are preferentially concentrated by the vortices. The results are indicated on table 1 (see also figures 5 and 6). They show that the optimal sizes lie between 1 and 50 cm in the region of the planets (for a bulk density  $\rho_s = 2g/cm^3$ ). Such particles are concentrated in the vortices after only one rotation period. By contrast, the capture time for particles of  $1\mu m$  in size (the initial size of the dust grains in the primordial nebula) is  $\Omega t_{capt} \sim 10^9$  (we have a similar characteristic value for their settling time). This exceeds the lifetime of a circumstellar disk by many orders of magnitude. These results (see also sections 3.4 and 4.5) indicate that sticking of particles up to cm-sized bodies is an indispensable step in the process of planet formation.

We can also study how the mass captured by the vortices varies throughout the nebula and how it depends on the size of the particles. According to equations (38) (42) and (44), the mass captured by a vortex during its lifetime can be written:

$$\frac{M_{life}}{M_{\oplus}} = 8.916 \cdot 10^{-4}(\Omega t_{life})r f^2(\xi) \quad (56)$$

where we have introduced the Earth mass  $M_{\oplus} = 5.976 \cdot 10^{27} g$  as a normalization factor.

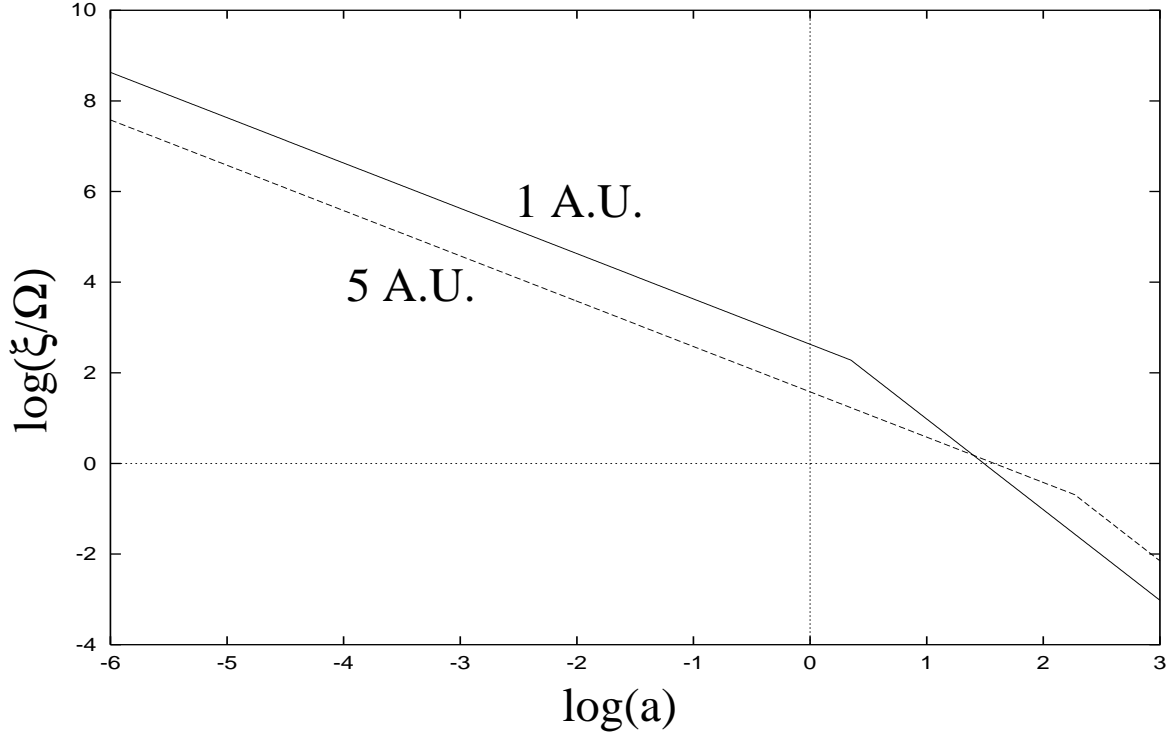


Figure 5: Variation of the friction parameter with the size of the particles at  $r = 1 \text{ A.U.}$  and  $r = 5 \text{ A.U.}$  (we have taken  $\rho_s = 2g/cm^3$ ). The capture is optimum for particles with friction parameter  $\xi \sim \Omega$ . This corresponds to decimetric sizes in the region of the planets.

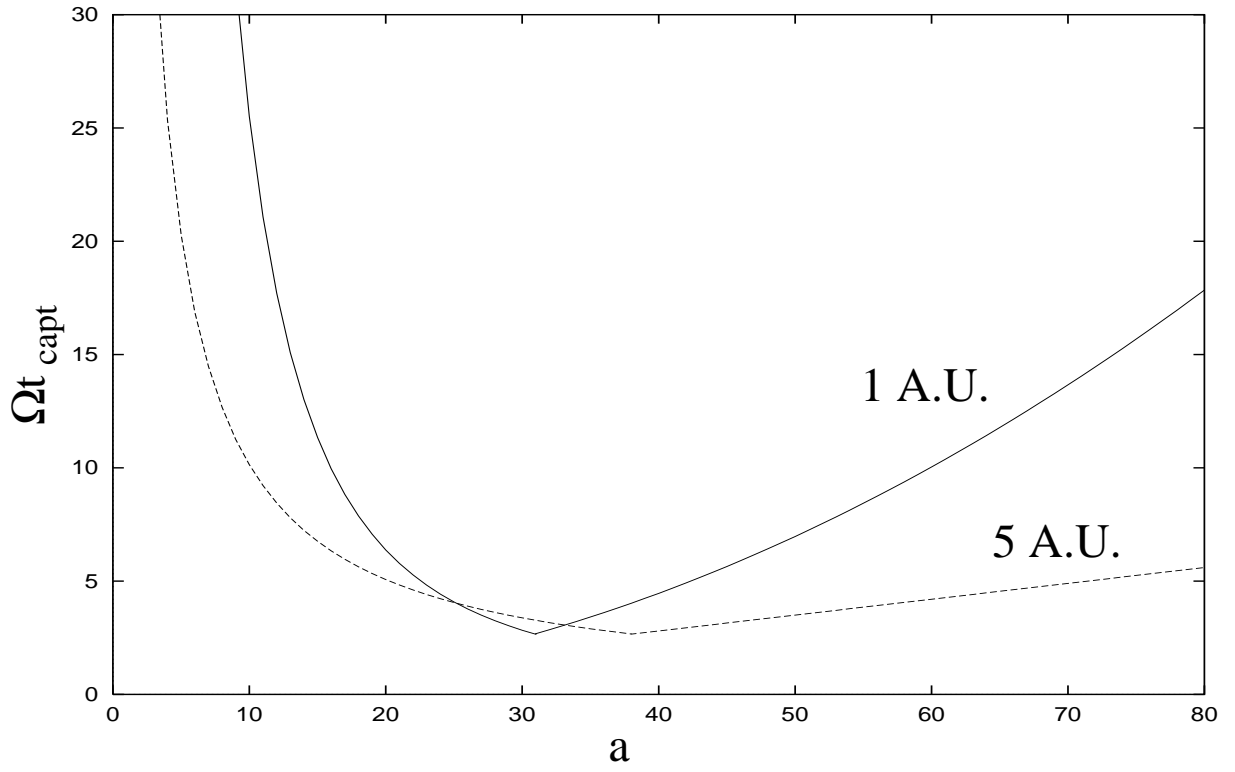


Figure 6: Variation of the capture time with the size of the the particles at  $r = 1 A.U$  and  $r = 5 A.U$  ( $\rho_s = 2g/cm^3$ ). The capture time is minimum for particles with radius  $a \sim 30cm$ .

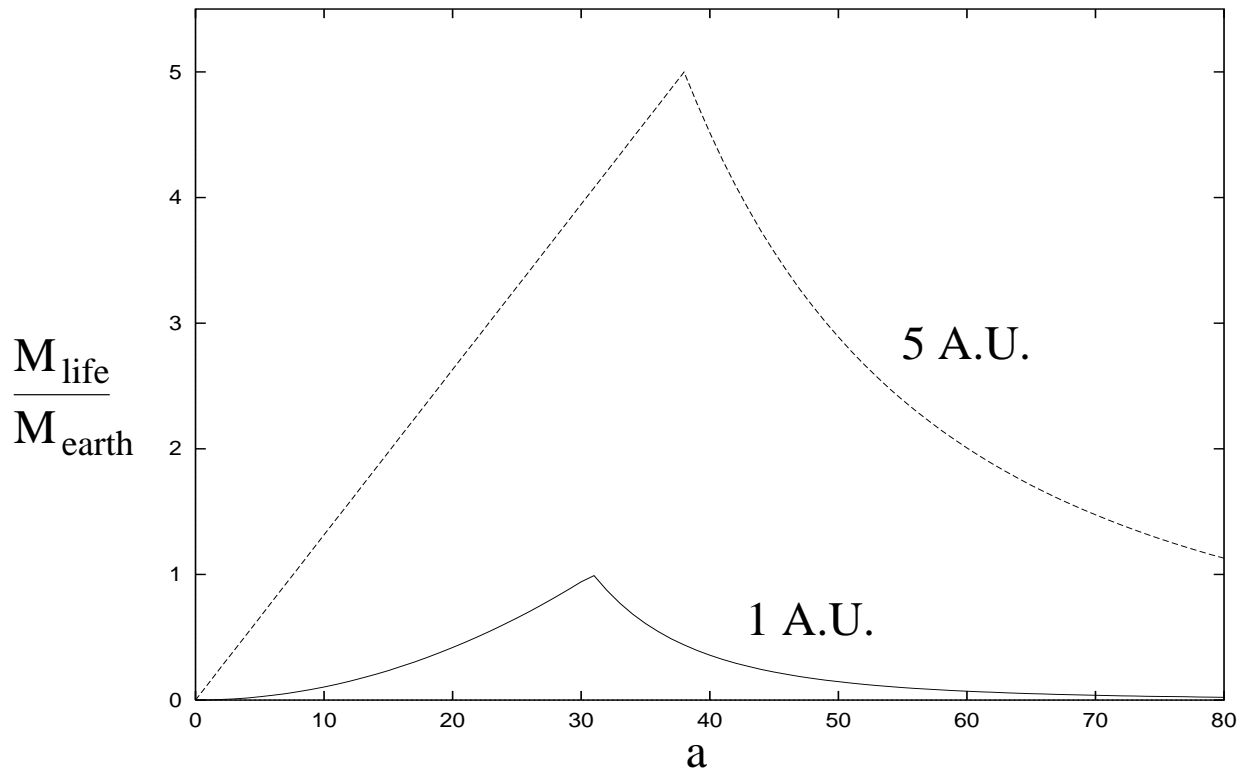


Figure 7: Variation of  $M_{\text{life}}$  with the size of the particles at  $r = 1 \text{ A.U.}$  and  $r = 5 \text{ A.U.}$  ( $\rho_s = 2\text{g/cm}^3$ ).

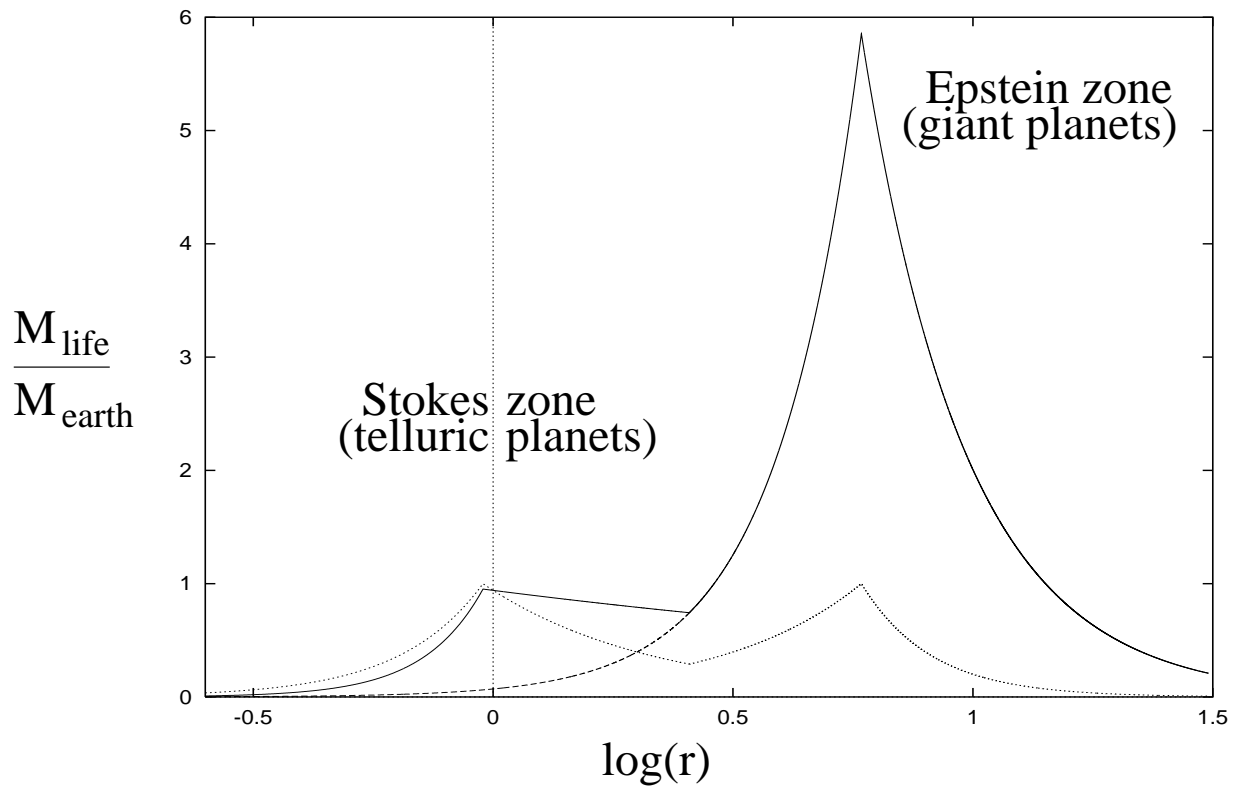


Figure 8: Variation of  $M_{\text{life}}$  with the heliocentric distance for particles with size  $a = 30\text{cm}$  and bulk density  $\rho_s = 2\text{g/cm}^3$ .

At  $r = 1A.U$  and for optimal particles with size  $a \sim 30cm$  and bulk density  $\rho_s \sim 2g/cm^3$  (see table 1), we have  $\xi \sim \Omega$  leading to  $rf^2 \sim 1$ . Since the vortex lifetime is not accurately known, it makes sense to calibrate its value so as to satisfy  $M_{life}(1A.U) = M_{\oplus}$ . This yields  $\Omega t_{life} \simeq 1122$ , corresponding to  $\sim 180$  rotation periods, in agreement with the estimate of Barge & Sommeria (1995) based on the value of the disk  $\alpha$ -viscosity and with the numerical simulations of Godon & Livio (1999a,b,c). Figure 7 shows how the mass  $M_{life}$  depends on the size of the particles at a given position of the solar nebula. We can also determine how it varies with the heliocentric distance for a given type of particles. The results are reported on figure 8 (full line) for particles with  $a \sim 30cm$  and  $\rho_s \sim 2g/cm^3$ . The captured mass presents a global maximum near Jupiter’s orbit and a plateau in the Earth’s region. These results complete the work of Barge & Sommeria (1995) who first noticed the existence of an optimum near Jupiter. However, they didn’t consider the Stokes regime in their article and made the wrong statement that “inside Jupiter’s orbit, particle concentration occurs in an annular region at the vortex periphery [because the friction parameter  $\xi$  is larger]”. In reality, the friction parameter decreases anew when we enter the Stokes domain at  $r < r_c$  (see figure 3). This allows the existence of *another* optimum near the Earth orbit. Therefore, the mass collected by the vortices in the inner zone is larger than one would obtain without this change of regime (the dash line in figure 8 would be found if the Epstein law was used in the whole disk). This transition may explain the division of the solar system in two groups of planets. Moreover, the vortex scenario explains naturally the disymmetry between these two groups: the mass capture rate is larger in the outer zone simply because the vortices are larger. Indeed, the captured mass is not only proportional to  $f^2$  (which would give the symmetrical dotted line of figure 8) but also to the product  $\sigma_d R^2$  which increases linearly with  $r$ . This effect may explain the difference in size and mass between telluric and giant planets. Moreover, the mass captured by the vortices in the outer zone should be larger than these estimates since they intercept in priority the matter drifting towards the sun. On the other hand, the intermediate region at  $\sim 3 A.U$  should be further depleted due to its proximity with the global maximum.

In conclusion, we find that there are two locations in the primordial nebula where the trapping of dust by vortices is optimal. These locations belong to the Stokes and to the Epstein zones and fall near the Earth and Jupiter’s orbit respectively. The zone of transition of the gas drag law is consistent with the position of the asteroid belt which marks the separation between telluric and giant planets. The asymmetry between the two groups of planets may be related to the size of the vortices which are bigger in the outer zone and therefore capture more mass. The exact values of  $r_{in}$ ,  $r_c$  and  $r_{out}$  depend on the spectrum of size of the particles, which is not well-known, but the W-shape of figures 4 and 8 is generic and agrees with the global structure of the solar system.

### 3 Stochastic motion of a particle in a vortex

#### 3.1 The diffusion equation

Due to small-scale turbulence, the motion of a particle in a vortex is not deterministic but *stochastic*. Turbulent fluctuations produce some kicks which progressively deviate the particle from its unperturbed trajectory. This is similar to what happens to a colloidal



particle in suspension in a liquid (Brownian motion). An individual fluctuation has a minute effect on the motion of the particle, but the repeated action of these fluctuations gives rise to a macroscopic process of diffusion. The effect of turbulence on the sedimentation of dust particles in the protoplanetary nebula has been considered in detail by Dubrulle *et al.* (1995). We use a similar approach to study the effect of turbulence on the capture of dust by large-scale vortices.

The transport equation governing the evolution of the dust surface density inside a vortex can be written:

$$\frac{\partial \sigma_d}{\partial t} + \nabla(\sigma_d \langle \mathbf{v} \rangle) = \nabla(D \nabla \sigma_d) \quad (57)$$

where  $\langle \mathbf{v} \rangle$  is the mean velocity of the particles and  $D$  their diffusivity. The mean velocity  $\langle \mathbf{v} \rangle$  is given by the deterministic model of section 2.3. According to equations (22)(23) or (27) (28), it can be written:

$$\langle \mathbf{v} \rangle = \mathbf{V} - \frac{1}{t_{capt}} \mathbf{r} \quad (58)$$

where  $\mathbf{V}$  corresponds to the pure rotation of the particles in the vortex and  $-\mathbf{r}/t_{capt}$  is their drift towards the center. In the case of light particles ( $\xi \gg \Omega$ ),  $\mathbf{V}$  is equal to the velocity of the vortex while in the case of heavy particles ( $\xi \ll \Omega$ ),  $\mathbf{V}$  is equal to the epicyclic velocity (see section 2.3). When (58) is substituted into (57), the diffusion equation takes the form:

$$\frac{\partial \sigma_d}{\partial t} + \nabla(\sigma_d \mathbf{V}) = \nabla \left( D \nabla \sigma_d + \frac{\sigma_d}{t_{capt}} \mathbf{r} \right) \quad (59)$$

The first term in the r.h.s is a pure diffusion due to small-scale turbulence and the second term is a drift toward the vortex center due to the combined effect of the Coriolis force and the vortex (anticyclonic) rotation. Equation (59) illustrates the bimodal nature of turbulence: the diffusion is due to small-scale fluctuations hardly affected by the rotation of the disk (3D turbulence) and the trapping process is a consequence of the Coriolis force and the existence of coherent structures in the disk (2D turbulence).

Since we are mainly interested by orders of magnitude and in order to avoid unnecessary mathematical complications, we shall consider from now on that the vortices are circular with typical radius  $R$ . In this approximation, we can restrict ourselves to axisymmetric solutions for which the advection term in equation (59) cancels out. We are led therefore to study the Fokker-Planck equation:

$$\frac{\partial \sigma_d}{\partial t} = \nabla \left( D \nabla \sigma_d + \frac{\sigma_d}{t_{capt}} \mathbf{r} \right) \quad (60)$$

For an initial condition consisting of a Dirac function centered at  $\mathbf{r}_0$ , there is a well-known analytical solution of equation (60):

$$\sigma_d = \frac{M}{2\pi D t_{capt} (1 - e^{-2t/t_{capt}})} e^{-\frac{(\mathbf{r}-\mathbf{r}_0)^2 e^{-t/t_{capt}}}{2D t_{capt} (1 - e^{-2t/t_{capt}})}} \quad (61)$$

where  $M$  is the total mass of particles contained in the vortex. This formula shows that the relaxation time is equal to the capture time  $t_{capt}$  not affected by turbulence.

The equilibrium solution of the Fokker-Planck equation (60) satisfies the condition:

$$D\nabla\sigma_d + \frac{\sigma_d}{t_{capt}}\mathbf{r} = 0 \quad (62)$$

expressing the balance between the diffusion and the drift. It corresponds to a gaussian density profile of the form:

$$\sigma_d = \sigma_d(0)e^{-\frac{r^2}{2Dt_{capt}}} \quad (63)$$

This is also the solution of equation (61) for  $t \rightarrow +\infty$ . In practice, the equilibrium distribution (63) is established for  $t \sim t_{capt}$ . Then, the particles are concentrated in the vortices on a typical length:

$$l_d = \sqrt{2Dt_{capt}} \quad (64)$$

### 3.2 Vertical sedimentation

Equation (60) is similar to the diffusion equation

$$\frac{\partial n_d}{\partial t} = \frac{\partial}{\partial z} \left( D \frac{\partial n_d}{\partial z} + \frac{\Omega^2}{\xi} n_d z \right) \quad (65)$$

used by Dubrulle *et al.* (1995) to describe the sedimentation of the dust particles and determine the sub-disk scale height (see also Weidenschilling 1980). The drift towards the vortex center is replaced in their study by the drift  $-\frac{\Omega^2}{\xi}z$  towards the ecliptic plane due to gravity. For light particles,  $t_{capt} \sim \frac{8\xi}{3\Omega^2}$  [see equation (33)] and the two equations coincide up to numerical factors. This implies that the particles are concentrated in the vortices on a length  $l_d$  comparable with the sub-disk scale height  $H_d$  determined by Dubrulle *et al.* (1995) [see their section 3].

It is relatively straightforward to include the vertical sedimentation of particles in our study, although we shall specialize in the following on their *horizontal* accumulation in vortices. Introducing the volume density  $\rho_d(r, z, t) = \frac{1}{H_d}n_d(z, t)\sigma_d(r, t)$  and using equations (60) and (65), we obtain:

$$\frac{\partial \rho_d}{\partial t} = \nabla \cdot \left\{ D\nabla\rho_d + \frac{\Omega^2}{\xi}\rho_d \left( \frac{3}{8}\mathbf{r}_\perp + \mathbf{z} \right) \right\} \quad (66)$$

where  $\mathbf{r}_\perp$  and  $\mathbf{z}$  are the component of  $\mathbf{r}$  in the directions perpendicular and parallel to the disk rotation vector  $\mathbf{\Omega}$ . Integrating equation (66) on the vertical direction returns equation (60) for the surface density.

### 3.3 Diffusivity of dust particles

It remains now to specify the value of the diffusion coefficient appearing in equation (60). In general, the turbulent viscosity of the gas is written under the form  $\nu \sim \alpha \frac{c_s^2}{\Omega}$  where  $c_s$  is the sound speed and  $\alpha$  a non dimensional parameter which measures the efficiency of turbulence (Shakura & Sunyaev 1973). Following current nebula models,  $10^{-4} < \alpha < 10^{-2}$ . When the turbulence is generated by differential rotation,  $\alpha = 2 \cdot 10^{-3}$  (Dubrulle 1992) and

we shall take this value for numerical applications. Since the disk height is  $H \sim c_s/\Omega$  (see equation (5)), the turbulent viscosity can be written  $\nu \sim \alpha H^2 \Omega$  or, alternatively,  $\nu \sim \alpha \Omega R^2$  where  $R$  is the vortex radius. More precisely, assuming a power law spectrum  $E(k) \sim k^{-\gamma}$  for the gas turbulence (with  $\gamma \simeq 5/3$ ), we have

$$\nu = \frac{\alpha \Omega R^2}{\sqrt{\gamma + 1}} \quad (67)$$

According to Dubrulle *et al.* (1995), the diffusivity of the particles can be written:

$$D = g(\xi) \nu \quad (68)$$

where

$$g(\xi) = \left( \frac{\xi}{\xi + \Omega} \frac{\text{Arctan}(B_{k_0})}{B_{k_0}} \right)^{1/2} \quad (69)$$

is a function of the friction parameter. The reduction factor of Völk *et al.* (1980):

$$B_{k_0} = \frac{k_0 v_s}{\xi + \Omega} \quad (70)$$

depends on the size  $k_0^{-1} \sim \sqrt{\alpha} H$  of the largest eddies of turbulence and on the systematic velocity  $v_s$  of the dust grains. In the vortices,  $v_s$  is equal to the drift velocity  $r/t_{\text{capt}}$ .

For light particles ( $\xi \gg \Omega$ ),  $g(\xi) \rightarrow 1$  and

$$D = \frac{\alpha \Omega R^2}{\sqrt{\gamma + 1}} \quad (\text{light particles}) \quad (71)$$

This result is expectable since light particles mainly follow the streamlines of the gas. Consequently, their diffusivity tends to the gas turbulent viscosity  $\nu$ .

For heavy particles ( $\xi \ll \Omega$ ),  $g(\xi) \rightarrow \sqrt{\xi/\Omega}$  and

$$D = \frac{\alpha \Omega R^2}{\sqrt{\gamma + 1}} \left( \frac{\xi}{\Omega} \right)^{1/2} \quad (\text{heavy particles}) \quad (72)$$

For  $\xi \rightarrow 0$ ,  $D \rightarrow 0$  since there is no coupling with the gas. For  $\xi \sim \Omega$ , equations (71) and (72) give the same result, so we can use these expressions in the whole range of friction parameters. Note, however, that the diffusion approximation is not strictly valid for heavy particles, so equation (72) must be taken with care.

Substituting equations (33)(34) and (71)(72) into equation (64), the concentration length can be written explicitly:

$$\frac{l_d}{R} = \left( \frac{16\alpha}{3\sqrt{\gamma + 1}} \right)^{1/2} \left( \frac{\xi}{\Omega} \right)^{1/2} \quad (\text{light particles}) \quad (73)$$

$$\frac{l_d}{R} = \left( \frac{16\alpha}{3\sqrt{\gamma + 1}} \right)^{1/2} \left( \frac{\Omega}{\xi} \right)^{1/4} \quad (\text{heavy particles}) \quad (74)$$

As expected, the concentration is optimum for  $\xi \sim \Omega$ . In that case, the particles are distributed over a length  $l_d \sim \sqrt{\alpha}R$ . Lighter and heavier particles are less concentrated. When

$$\frac{\xi}{\Omega} > \frac{3\sqrt{\gamma+1}}{16\alpha} \simeq 153 \quad (75)$$

or

$$\frac{\xi}{\Omega} < \left( \frac{16\alpha}{3\sqrt{\gamma+1}} \right)^2 \simeq 4 \cdot 10^{-5} \quad (76)$$

the drift is negligible and there is no concentration ( $l_d > R$ ).

### 3.4 Application to the solar nebula

We now apply these results to the case of the solar nebula and show how the vortex scenario can make possible the formation of planetesimals at certain preferred locations of the disk.

It is generally believed that planetesimals formed by the gravitational instability of the particle sublayer (Safronov 1969, Goldreich & Ward 1973). The dispersion relation for an infinite uniformly rotating sheet of gas is (see, e.g, Binney & Tremaine 1987):

$$\omega^2 = k^2 c_d^2 + 4\Omega^2 - 2\pi G\sigma_d k \quad (77)$$

where  $\sigma_d$  is the unperturbed surface density of the particles and  $c_d$  their velocity dispersion. The particle sub-layer (which behaves as a very compressible fluid) will be unstable provided that  $\omega^2 < 0$ , for some  $k$ . From equation (77), we obtain the criterion for gravitational instability (Toomre, 1964):

$$c_d < \frac{\pi G\sigma_d}{2\Omega} = V_{crit} \quad (78)$$

Once instability is triggered, the system crumbles into numerous planetesimals of order 10 km in size. Moreover, the growth time of density perturbation is predicted to be short, of the order of an orbital period. In addition, the instability criterion gives the impression that its operation does not require any sticking mechanism. Goldreich & Ward (1973) state that "...the fate of planetary accretion no longer appears to hinge on the stickiness of the surface of dust particles". This is very attractive because sticking mechanisms are relatively *ad hoc* and ill-understood. For these reasons (and also for a lack of alternatives), the Safronov-Goldreich-Ward scenario was nearly universally accepted as the key mechanism for forming planetesimals. Therefore, a swarm of bodies of a few km in diameter was a common starting point for numerical simulations of planetary formation.

However, Weidenschilling (1980), followed by Cuzzi *et al.* (1993) and Dubrulle *et al.* (1995), realized that this simplistic picture was ruled out if the primordial nebula was turbulent. Indeed, turbulence reduces considerably the vertical sedimentation of the dust particles and prevents gravitational instability. According to equations (41) and (42), the velocity threshold imposed by the instability criterion (78) is of order  $V_{crit} = 5\text{cm/s}$  throughout the nebula. Even if the nebula as a whole was perfectly laminar, the formation of a dense layer of particles (considered as a heavy fluid) would create a turbulent shear with the overlying gas (see, e.g., Weidenschilling & Cuzzi 1993). The velocity dispersion of the particles can be estimated by  $c_d \sim \sqrt{\alpha}c_s$  and easily reaches several *meters* per second (when a numerical value is needed, we shall take  $c_d = 5\text{m/s}$ ). Therefore, the instability

criterion (78) is not satisfied (see appendix B for a rigorous derivation of this criterion in a turbulent disk). Turbulence is responsible for too high velocity dispersions or, alternatively, the surface density of the dust sublayer is not sufficient to trigger the gravitational instability. The density needs to be increased by a factor  $A_c \sim 100$  or more to overcome the threshold imposed by Toomre instability criterion.

There is therefore a major problem to form planetesimals by gravitational instability in a turbulent disk. As first suggested by Barge & Sommeria (1995), the presence of vortices in the disk can solve this problem. Indeed, by capturing and concentrating the particles, the vortices can increase locally the surface density of the dust sublayer and initiate the gravitational instability. Let us first discuss the *concentration* effect. Inside a vortex, an initial mass of order  $\sigma_d \pi R^2$  is concentrated on a typical length  $l_d$  given by equation (64). The surface density is therefore amplified by a factor  $(R/l_d)^2$  depending on the size of the particles. Using equations (73)(74), this amplification can be written explicitly

$$\left(\frac{\sigma_d^{vort}}{\sigma_d}\right)_{conc.} = \frac{3}{16\alpha} \sqrt{\gamma+1} \frac{\Omega}{\xi} \quad (\text{light particles}) \quad (79)$$

$$\left(\frac{\sigma_d^{vort}}{\sigma_d}\right)_{conc.} = \frac{3}{16\alpha} \sqrt{\gamma+1} \left(\frac{\xi}{\Omega}\right)^{1/2} \quad (\text{heavy particles}) \quad (80)$$

The amplification is maximum for  $\xi \sim \Omega$  and takes the value  $A_{max}^{conc.} = \frac{3}{16\alpha} \sqrt{\gamma+1} \simeq 150$ . As we have seen in section 2.5, this corresponds to particles of size  $a = 30cm$  and bulk density  $\rho_d = 2g/cm^3$  in the regions of the Earth and Jupiter. This enhancement is sufficient to satisfy the instability criterion (78)<sup>5</sup>. For microscopic particles, on the contrary, there is no density enhancement. In that case,  $l_d \sim 10^3 R$  (in the region of the planets) and the particles rapidly diffuse away from the vortices (see section 4.5). Gravitational instability will be possible provided that:

$$\frac{\xi}{\Omega} < \frac{3}{16\alpha} \sqrt{\gamma+1} \frac{1}{A_c} \simeq 1.53 \quad (81)$$

On table 1, we report, as a function of the heliocentric distance, the minimum size of the particles which satisfy this criterion (see also figures 5 and 9). These results indicate that particles must have grown up to some centimeters to trigger the gravitational instability. Therefore, sticking processes are needed to reach this range of sizes (recall that this was claimed to be not necessary in the initial Safronov-Goldreich-Ward scenario).

In conclusion, by allowing a local enhancement of the particle surface density, the vortices can favour the formation of planetesimals by gravitational instability. This rehabilitates the Safronov-Goldreich-Ward theory at certain preferred locations of the disk (i.e inside the vortices) and for sufficiently large (decimetric) particles. A sufficient enhancement is achieved simply by the horizontal *concentration* of the dust layer in the vortex (a process similar to the vertical sedimentation). However, this mechanism alone is not sufficient to produce enough planetesimals to form the planets. The vortices must also *capture* the

---

<sup>5</sup>We can argue that when  $l_d$  is comparable to the sub-disk thickness  $H_d$ , the instability criterion derived in the case of a thin disk is not applicable anymore. However, according to Jeans criterion, a volume element of size  $H_p$  and mass  $M_p$  is unstable if the velocity dispersion of the particles  $c_d^2$  is less than their potential energy  $\frac{GM_d}{H_d}$ . Since  $c_d \sim H_d \Omega$  and  $M_d \sim \sigma_d H_d^2$ , this condition returns the criterion (78).

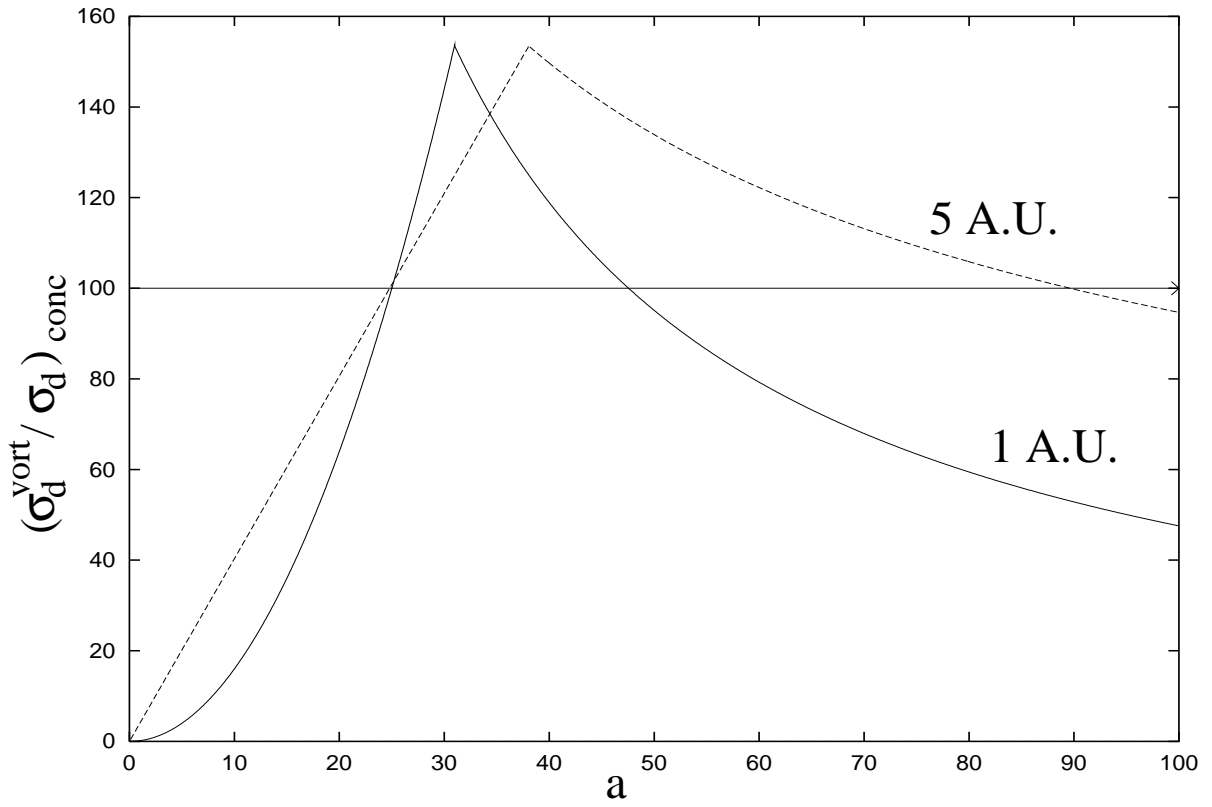


Figure 9: Enhancement of the dust surface density inside the vortices (due to concentration) as a function of the size of the particles at  $r = 1A.U$  and  $r = 5A.U$  ( $\rho_s = 2g/cm^3$ ).

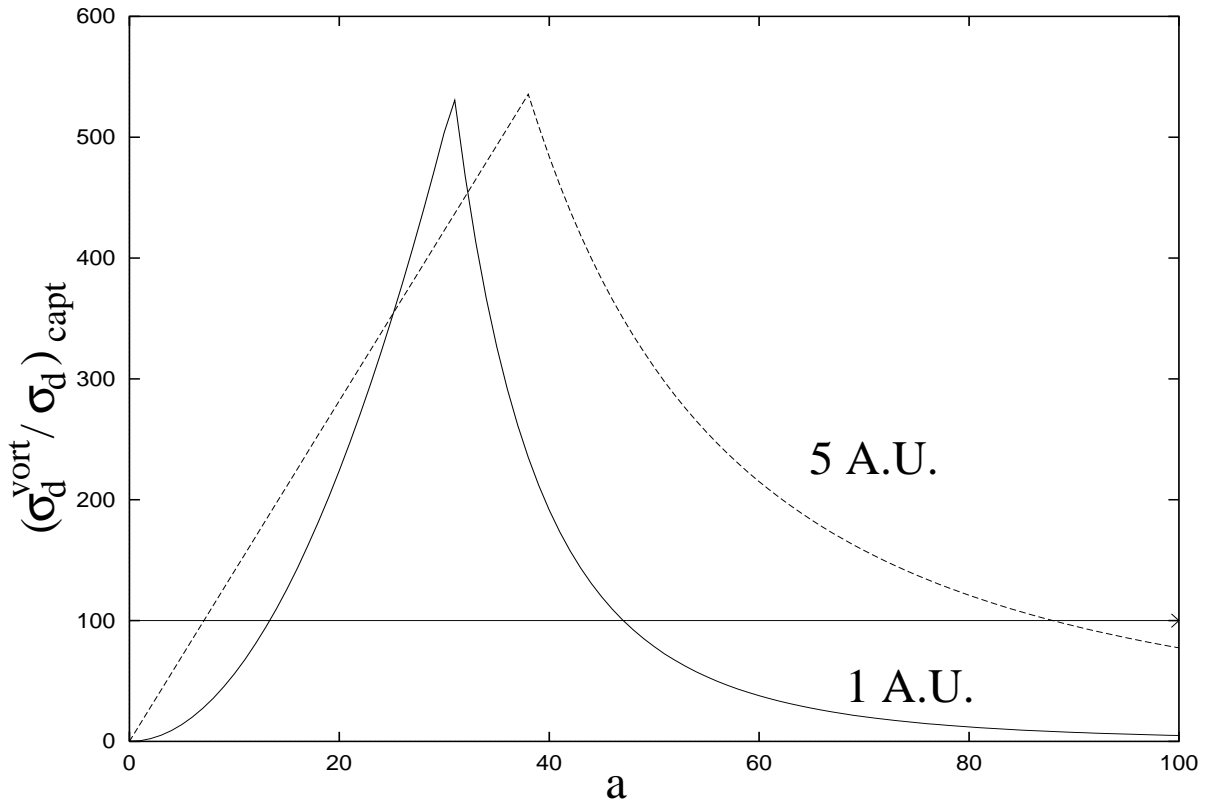


Figure 10: Enhancement of the dust surface density inside the vortices (due to capture) as a function of the size of the particles at  $r = 1A.U$  and  $r = 5A.U$  ( $\rho_s = 2g/cm^3$ ).

surrounding mass. This is another source for density enhancement (Barge & Sommeria 1995). Returning to equation (38), we find that the average surface density of the particles collected by a vortex during its lifetime is

$$\left(\frac{\langle\sigma_d^{vort}\rangle}{\sigma_d}\right)_{capt.} = \frac{3}{2\pi}(\Omega t_{life})f^2(\xi) \quad (82)$$

with  $\Omega t_{life} \sim 1122$  (see section 2.5). The maximum amplification, reached by particles with  $\xi \sim \Omega$ , is  $A_{max}^{capt.} = \frac{3}{2\pi}(\Omega t_{life}) \simeq 536$  a little bit larger than the previous value (recall however that  $t_{life}$  is not known precisely). Gravitational instability will be possible for particles whose friction parameter satisfies

$$\frac{\xi}{\Omega} < \frac{3}{2\pi}(\Omega t_{life})\frac{1}{A_c} \simeq 5.4 \quad (83)$$

See also table 1 and figures 5, 10 for the same criterion expressed in terms of the size of the particles.

If we now take into account both the concentration effect and the capture process, we obtain an amplification

$$\frac{\sigma_d^{vort}}{\sigma_d} = \frac{M_{life}}{\sigma_d \pi l_d^2} = \left(\frac{\sigma_d^{vort}}{\sigma_d}\right)_{conc.} \left(\frac{\langle\sigma_d^{vort}\rangle}{\sigma_d}\right)_{capt.} \quad (84)$$

with a maximum value  $A_{max} = A_{max}^{conc.} A_{max}^{capt.} \sim 10^5$ . The range of particles which can collapse is enlarged:

$$\frac{\xi}{\Omega} < \left(\frac{9}{32\pi} \frac{\sqrt{\gamma+1}}{\alpha} (\Omega t_{life}) \frac{1}{A_c}\right)^{1/2} \simeq 28.6 \quad (85)$$

but, even in this optimistic situation, the particles must have reached relatively large sizes to trigger the gravitational instability (see table 1). Of course, if the vortex lifetime is increased, smaller particles have the possibility to collapse since the vortex captures more mass. In fact, this is not completely correct because the previous results assume that the escape of particles due to turbulent fluctuations can be neglected. This is not always the case (in particular for small particles) and this problem is now considered in detail.

## 4 The rate of escape

### 4.1 Formulation of the problem

The diffusion equation (60) is similar, in structure, with the Kramers-Chandrasekhar equation:

$$\frac{\partial f}{\partial t} = \frac{\partial}{\partial \mathbf{v}} \left( D \frac{\partial f}{\partial \mathbf{v}} + \xi f \mathbf{v} \right) \quad (86)$$

introduced in the case of colloidal suspensions and in stellar dynamics (Kramers 1940, Chandrasekhar 1943a,b). In this equation,  $f(\mathbf{v}, t)$  governs the velocity distribution of the particles in the system. The first term in the r.h.s is a pure diffusion and the second term is a *dynamical friction*. These terms model the encounters between stars or the collisions



between the colloidal particles and the fluid molecules. Comparing equations (60) and (86), we see that the position in (60) plays the role of the velocity in (86) and the capture time  $t_{capt}$  the role of the friction time  $\xi^{-1}$ . In particular the friction force and the drift term are *linear* in  $\mathbf{v}$  and  $\mathbf{r}$  respectively. Equation (86) was used by Chandrasekhar (1943b) to study the evaporation of stars in globular clusters (this is similar to the Kramers problem for the escape of colloidal suspensions over a potential barrier). Due to collisions, some stars may acquire very high energies and escape from the system (being ultimately captured by the gravity of nearby objects). Similarly, in our situation, turbulent fluctuations allow some dust particles to diffuse towards higher and higher radii and finally leave the vortex (being eventually transported by the local Keplerian shear). In each case, the friction force or the drift acts against the diffusion and can reduce significantly the escape process.

We try now to evaluate the rate of particles that leave the vortex on account of turbulent fluctuations. To that purpose, we formulate the problem in terms of the density probability  $W(\mathbf{r}, t) = W(|\mathbf{r}|, t)$  that a particle located initially in the annulus between  $|\mathbf{r}| = r_0$  and  $r_0 + dr_0$  will be found in the surface element around  $\mathbf{r}$  at time  $t$ . According to equation (60), the time evolution of the probability  $W(\mathbf{r}, t)$  is given by

$$\frac{\partial W}{\partial t} = \nabla \left( D \nabla W + \frac{W}{t_{capt}} \mathbf{r} \right) \quad (87)$$

with initial condition

$$W(\mathbf{r}, t) = \frac{\delta(|\mathbf{r}| - r_0)}{2\pi r_0} \quad \text{as } t \rightarrow 0 \quad (88)$$

where  $\delta$  stands for Dirac's  $\delta$ -function. We assume that when the particle reaches the vortex boundary at  $|\mathbf{r}| = R$ , it is immediately transported away by the Keplerian shear. In other words, we adopt the boundary condition:

$$W(\mathbf{r}, t) = 0 \quad \text{for } |\mathbf{r}| = R \quad \text{for all } t > 0 \quad (89)$$

We call

$$\mathbf{J} = - \left( D \nabla W + \frac{W}{t_{capt}} \mathbf{r} \right) \quad (90)$$

the current of probability, i.e  $\mathbf{J} dl \hat{\mathbf{n}}$  gives the probability that a particle crosses an element of length  $dl$  between  $t$  and  $t + dt$  ( $\hat{\mathbf{n}}$  is a unit vector normal to the element of length under consideration).

We first introduce the probability  $p(r_0, t) dt$  that a particle located initially in the annulus between  $|\mathbf{r}| = r_0$  and  $r_0 + dr_0$  reaches for the first time the vortex boundary between  $t$  and  $t + dt$ . According to what was just said concerning the interpretation of (90), we have:

$$p(r_0, t) = \oint_{|\mathbf{r}|=R} \mathbf{J} \hat{\mathbf{n}} dl = - \left( 2\pi D r \frac{\partial W}{\partial r} \right)_{r=R} \quad (91)$$

The total probability  $Q(r_0, t)$  that the particle has reached the vortex boundary between 0 and  $t$  is

$$Q(r_0, t) = \int_0^t p(r_0, t') dt' \quad (92)$$

Finally, we average  $Q(r_0, t)$  over an appropriate range of initial positions in order to get the expectation  $Q(t)$  that the particle has left the vortex at time  $t$ . We have

$$Q(t) = \int Q(r_0, t) \mu(r_0) 2\pi r_0 dr_0 \quad (93)$$

where  $\mu(|\mathbf{r}_0|)$  governs the initial probability distribution of the particles in the vortex. In terms of the function  $Q$ , the rate of escape of the particles can be written

$$\frac{1}{t_{esc}} = \frac{1}{(1-Q)} \frac{dQ}{dt} \quad (94)$$

As mentioned already, this problem is similar to the diffusion of colloidal suspensions over a potential barrier or to the evaporation of stars in globular clusters. As will soon become apparent, it reduces to solving a pseudo Schrödinger equation for a quantum oscillator in a “box”. In this analogy, the rate of escape appears to be related to the fundamental eigenvalue of the quantum problem. An explicit expression for the rate of escape can be obtained in two limits: when  $\xi \rightarrow 0$  or  $\xi \rightarrow \infty$ , the drift term can be ignored and the Fokker-Planck equation reduces to a pure diffusion equation (section 4.2). On the other hand, when  $\xi \simeq \Omega$ , the drift term is dominant and a perturbation approach inspired by the work of Sommerfeld and Chandrasekhar can be implemented to determine the ground state of the artificially limited quantum oscillator (sections 4.3 and 4.4).

## 4.2 The rate of escape when the drift term is ignored

When the drift term can be ignored (i.e for very light or very heavy particles, see inequalities (75)(76)), the Fokker-Planck equation (87) reduces to a pure diffusion equation

$$\frac{\partial W}{\partial t} = D \Delta W \quad (95)$$

which has to be solved in a circular domain with boundary conditions (88) and (89). The solution of this classical problem is

$$W = \frac{1}{\pi R^2} \sum_{n=1}^{+\infty} \frac{1}{J_1^2(\alpha_{0n})} J_0\left(\alpha_{0n} \frac{r_0}{R}\right) \times J_0\left(\alpha_{0n} \frac{r}{R}\right) e^{-\frac{D\alpha_{0n}^2}{R^2} t} \quad (96)$$

where  $J_m$  is Bessel function of order  $m$  and the  $\alpha_{0n}$ 's denote the roots of Bessel function  $J_0$ . The probability  $p(r_0, t)$  that a particle with an initial position  $r_0$  has reached the vortex boundary between  $t$  and  $t + dt$  is

$$p(r_0, t) = \frac{2D}{R^2} \sum_{n=1}^{+\infty} \frac{\alpha_{0n}}{J_1(\alpha_{0n})} J_0\left(\alpha_{0n} \frac{r_0}{R}\right) e^{-\frac{D\alpha_{0n}^2}{R^2} t} \quad (97)$$

and the total probability that the particle has escaped during the interval  $(0, t)$  is

$$Q(r_0, t) = 2 \sum_{n=1}^{+\infty} \frac{1}{\alpha_{0n} J_1(\alpha_{0n})} J_0\left(\alpha_{0n} \frac{r_0}{R}\right) \times \left(1 - e^{-\frac{D\alpha_{0n}^2}{R^2}t}\right) \quad (98)$$

Averaging the foregoing expression over all  $r_0$ 's in the range  $[0, R]$  with equal probability  $\mu(\mathbf{r}_0) = 1/\pi R^2$  (this corresponds to an initially homogeneous distribution of particles in the vortex), we obtain

$$Q(t) = 4 \sum_{n=1}^{+\infty} \frac{1}{\alpha_{0n}^2} \left(1 - e^{-\frac{D\alpha_{0n}^2}{R^2}t}\right) \quad (99)$$

To sufficient accuracy, we can keep only the first term in the series. The expectation that the particle has left the vortex at time  $t$  is therefore:

$$Q(t) \simeq \frac{4}{\alpha_{01}^2} \left(1 - e^{-\frac{D\alpha_{01}^2}{R^2}t}\right) \quad (100)$$

Since  $\alpha_{01} \simeq 2.40482\dots$ , this term represents  $\sim 70\%$  of the value of the series (99) and the approximation (100) is reasonable.

In conclusion, when the drift term is ignored, we find that the escape time is

$$t_{esc} = \frac{R^2}{D\alpha_{01}^2} \quad (101)$$

It corresponds, typically, to the time needed by the particles to diffuse over a distance  $\sim R$ , the vortex size. For light particles, using (71), we obtain explicitly

$$\Omega t_{esc} = \frac{\sqrt{\gamma+1}}{\alpha_{01}^2 \alpha} \quad (\text{light particles}) \quad (102)$$

and for heavy particles

$$\Omega t_{esc} = \frac{\sqrt{\gamma+1}}{\alpha_{01}^2 \alpha} \left(\frac{\Omega}{\xi}\right)^{1/2} \quad (\text{heavy particles}) \quad (103)$$

We shall come back to these expressions in section 4.5.

### 4.3 The effective Schrödinger equation

We now return to the general problem for the rate of escape when proper allowance is made for the drift. We find it convenient to introduce the notations

$$\tau = \frac{t}{t_{capt}} \quad \text{and} \quad \boldsymbol{\rho} = \frac{1}{\sqrt{2Dt_{capt}}} \mathbf{r} \quad (104)$$

or, in words, the time is measured in terms of the capture time and the distances are normalized by the concentration length (64). We let also:

$$w = 2Dt_{capt}W \quad (105)$$

and

$$\rho_\infty = \frac{1}{\sqrt{2Dt_{capt}}}R \quad (106)$$

In terms of these new variables, the problem (87)(88) and (89) takes the form:

$$\frac{\partial w}{\partial \tau} = \frac{1}{2}\Delta w + \nabla(w\rho) \quad (107)$$

$$w(\boldsymbol{\rho}, \tau) = \frac{\delta(\rho - \rho_0)}{2\pi\rho_0} \quad \text{as } \tau \rightarrow 0 \quad (108)$$

$$w(\boldsymbol{\rho}, \tau) = 0 \quad \text{for } \rho = \rho_\infty \quad \text{for all } \tau > 0 \quad (109)$$

With the change of variables

$$w = \psi e^{-\rho^2/2} \quad (110)$$

we can transform the Fokker-Planck equation (107) into a Schrödinger equation (with imaginary time) for a quantum oscillator:

$$\frac{\partial \psi}{\partial \tau} = \frac{1}{2}\Delta \psi + (1 - \frac{1}{2}\rho^2)\psi \quad (111)$$

However, contrary to the standard quantum problem, equation (111) has to be solved in a bounded domain of size  $\rho_\infty$  with the boundary condition (109). In other words, our problem consists in determining the characteristic functions of a quantum oscillator in a “box”.

First, we notice that a separation of the variables can be effected by the substitution

$$\psi = \phi(\rho)e^{-\lambda\tau} \quad (112)$$

where  $\lambda$  is, for the moment, an unspecified constant. This transformation reduces the Schrödinger equation in a second order ordinary differential equation:

$$\frac{d^2\phi}{d\rho^2} + \frac{1}{\rho}\frac{d\phi}{d\rho} + (2 + 2\lambda - \rho^2)\phi = 0 \quad (113)$$

Let  $\{\phi_n\}$  be the solutions of this differential equation satisfying the boundary condition  $\phi_n(\rho_\infty) = 0$  and  $\lambda_n$  the corresponding eigenvalues. The eigenfunctions form a complete set of orthogonal functions for the scalar product

$$\langle fg \rangle = \int_0^{\rho_\infty} f(\rho)g(\rho)2\pi\rho d\rho \quad (114)$$

This system can be further normalized, i.e  $\langle \phi_n \phi_m \rangle = \delta_{nm}$ . Any function  $f(\rho)$  satisfying the boundary condition (109) can be expanded on this basis, and we have the formula:

$$f(\rho) = \sum_n \langle f \phi_n \rangle \phi_n \quad (115)$$

In particular:

$$\delta(\rho - \rho_0) = \sum_n 2\pi\rho_0\phi_n(\rho_0)\phi_n(\rho) \quad (116)$$

The general solution of the problem (107) (109) can be expressed in the form

$$w(\rho, \tau) = \sum_n A_n e^{-\lambda_n \tau} e^{-\rho^2/2} \phi_n(\rho) \quad (117)$$

where the coefficients  $A_n$  are determined by the initial condition (108), using the expansion (116) for the  $\delta$ -function. We obtain:

$$w(\rho, \tau) = e^{-(\rho^2 - \rho_0^2)/2} \sum_n e^{-\lambda_n \tau} \phi_n(\rho)\phi_n(\rho_0) \quad (118)$$

Using the foregoing solution for  $w$ , the probability that a particle initially located at  $\rho_0$  leaves the vortex between  $\tau$  and  $\tau + d\tau$  is [see Eq. (91)]:

$$\begin{aligned} p(\rho_0, \tau) &= -\pi\rho_\infty e^{-(\rho_\infty^2 - \rho_0^2)/2} \\ &\times \sum_n e^{-\lambda_n \tau} \frac{d\phi_n}{d\rho}(\rho_\infty)\phi_n(\rho_0) \end{aligned} \quad (119)$$

The probability  $Q(\rho_0, \tau)$  that the particle has left the vortex at time  $\tau$  is therefore [see Eq. (92)]:

$$\begin{aligned} Q(\rho_0, \tau) &= -\pi\rho_\infty e^{-(\rho_\infty^2 - \rho_0^2)/2} \\ &\times \sum_n \frac{1 - e^{-\lambda_n \tau}}{\lambda_n} \frac{d\phi_n}{d\rho}(\rho_\infty)\phi_n(\rho_0) \end{aligned} \quad (120)$$

Finally, to obtain  $Q(\tau)$ , we have to take the average of the foregoing expression over the relevant range of  $\rho_0$ . To make the solution explicit, it remains to determine the eigenfunctions  $\phi_n$  and eigenvalues  $\lambda_n$  of the quantum oscillator.

#### 4.4 The ground state of the quantum oscillator

The dependance of the eigenvalues  $\lambda_n$  on the size of the “box” can be obtained from a procedure developed by Sommerfeld in his studies of the Kepler problem and the problem of the rotator in the quantum theory with “artificial” boundary conditions (Sommerfeld & Welker 1938, Sommerfeld & Hartmann 1940). This was used later on by Chandrasekhar (1943) to determine the rate of escape of stars from globular clusters, from which our study is inspired.

With the change of variables

$$x = \rho^2 \quad (121)$$

equation (113) becomes:

$$x \frac{d^2\phi}{dx^2} + \frac{d\phi}{dx} + \left( \frac{1}{2} + \frac{\lambda}{2} - \frac{x}{4} \right) \phi = 0 \quad (122)$$

Another change of variables:

$$\phi = f e^{-x/2} \quad (123)$$

transforms equation (122) into Kummer's equation

$$x \frac{d^2 f}{dx^2} + (1-x) \frac{df}{dx} + \frac{\lambda}{2} f = 0 \quad (124)$$

In the case of a “free” oscillator ( $\rho_\infty \rightarrow \infty$ ), it is well-known that the eigenvalues are  $\lambda_n = 2n$  (with  $n = 0, 1, \dots$ ) and the eigenfunctions are proportional to Laguerre polynomials  $f_n = AL_n^{(0)}$ . In a bounded domain ( $\rho_\infty < \infty$ ), the eigenvalues will be different but if  $\rho_\infty$  is sufficiently large, we expect that the difference will be small. Therefore, we expect  $\lambda_n \simeq 2n$ . Accordingly, for values of  $\tau$  of the order of unity, or greater, the first term in the series (120) will provide ample accuracy. Thus

$$Q(\rho_0, \tau) \simeq -\pi \rho_\infty e^{-(\rho_\infty^2 - \rho_0^2)/2} \times \frac{1}{\lambda_0} (1 - e^{-\lambda_0 \tau}) \frac{d\phi_0}{d\rho}(\rho_\infty) \phi_0(\rho_0) \quad (125)$$

We have therefore to determine the *ground state* of our artificially limited quantum oscillator. To that purpose, we expand  $f$  in a series:

$$f = \sum_n a_n x^n \quad (126)$$

and substitute this expansion into equation (124). Identifying term by term, we obtain the recursion formula:

$$a_{n+1} = \frac{n - \frac{\lambda}{2}}{(n+1)^2} a_n \quad (127)$$

which is easily reduced to

$$a_n = \frac{(n-1 - \frac{\lambda}{2})(n-2 - \frac{\lambda}{2}) \dots (-\frac{\lambda}{2})}{(n!)^2} a_0 \quad (128)$$

We know already that the eigenvalue  $\lambda_0$  of our artificial quantum oscillator is very small. Keeping only terms of order  $\lambda_0$  in the products (128), we obtain:

$$\begin{aligned} a_n &\simeq \frac{(n-1)(n-2) \dots 1 (-\frac{\lambda_0}{2})}{(n!)^2} a_0 \\ &= -\frac{(n-1)! \lambda_0}{(n!)^2} a_0 = -\frac{a_0 \lambda_0}{n! n} \end{aligned} \quad (129)$$

The ground state function can therefore be written

$$f_0(x) = a_0 (1 - \frac{\lambda_0}{2} \chi(x)) \quad (130)$$

with

$$\chi(x) = \sum_{n=1}^{+\infty} \frac{x^n}{n! n} = E_i(x) - \ln x - \gamma \quad (131)$$

where

$$E_i(x) = P \int_{-\infty}^x \frac{e^t}{t} dt \quad (132)$$

is the Exponential integral and  $\gamma = 0.577215\dots$  the Euler constant. The function  $\chi(x)$  is plotted on figure 11. The fundamental eigenvalue  $\lambda_0$  is determined by the condition  $f_0(\rho_\infty^2) = 0$ , i.e

$$\lambda_0 = \frac{2}{\chi(\rho_\infty^2)} \quad (133)$$

Returning to the original eigenfunction  $\phi_0(\rho)$ , we have established that

$$\phi_0(\rho) = a_0 \left(1 - \frac{\lambda_0}{2} \chi(\rho^2)\right) e^{-\rho^2/2} \quad (134)$$

where  $a_0$  is a normalizing factor. The final result can therefore be expressed in the form:

$$Q(\tau) = A(1 - e^{-\lambda_0 \tau}) \quad (135)$$

with

$$A = -\frac{\pi \rho_\infty}{\lambda_0} e^{-\rho_\infty^2/2} \frac{d\phi_0}{d\rho}(\rho_\infty) \overline{e^{\rho_0^2/2} \phi_0(\rho_0)} \quad (136)$$

In the expression for the amplitude, the bar indicates an average over the relevant range of  $\rho_0$ . In practice,  $A$  is close to unity but its precise value determines to which accuracy the approximation consisting in keeping only the dominant term in the series (120) is justified. For sufficiently large  $\rho_\infty$ 's, this will always be the case, so we shall take

$$Q(\tau) \simeq 1 - e^{-\lambda_0 \tau} \quad (137)$$

This expression is consistent with the physical condition  $Q(\tau) \rightarrow 1$  as  $\tau \rightarrow \infty$ .

## 4.5 Application to the solar nebula

Let  $M_0$  denote the total mass of particles present in the vortex at time  $t = 0$ . If we assume no renewal from the outside then, on account of turbulent fluctuations, some particles will escape the vortex and, according to equation (137), the mass will decay like:

$$M(t) = M_0 e^{-\lambda_0 t / t_{capt}} \quad (138)$$

The ‘‘evaporation’’ will take place on a typical time

$$t_{esc} = \frac{1}{\lambda_0} t_{capt} \quad (139)$$

where  $\lambda_0$  is given by equation (133). Note that both  $\lambda_0$  and  $t_{capt}$  depend on the friction parameter  $\xi$  of the particles. For very light or very heavy particles,  $\rho_\infty \rightarrow 0$  and  $\lambda_0 \simeq 2/\rho_\infty^2$ . With the definition (106) we find:

$$t_{esc} = \frac{R^2}{4D} \quad (140)$$

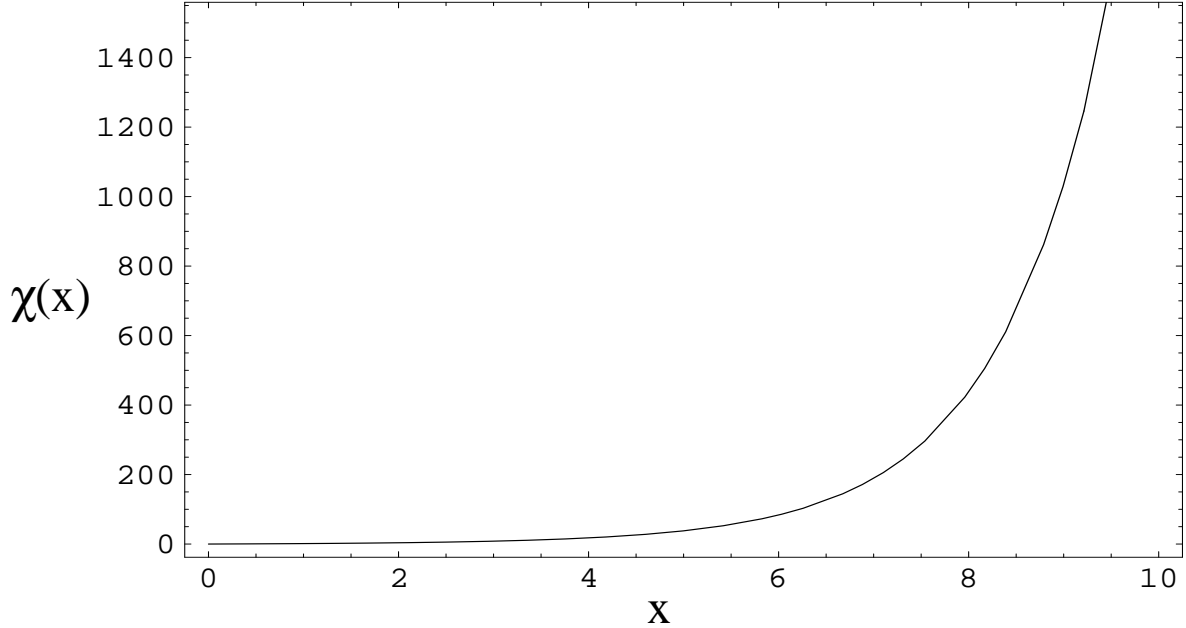


Figure 11: The function  $\chi(x)$ .

in good agreement with the result (101) obtained when the drift term is ignored. This shows that equation (139) can be used with good accuracy for all types of particles. Substituting equations (73)(74) and (33)(34) into equation (139), we obtain explicitly:

$$\Omega t_{esc} = \frac{4}{3} \frac{\xi}{\Omega} \chi \left( \frac{3\sqrt{\gamma+1}}{16\alpha} \frac{\Omega}{\xi} \right) \quad (\text{light particles}) \quad (141)$$

$$\Omega t_{esc} = \frac{4}{3} \frac{\Omega}{\xi} \chi \left( \frac{3\sqrt{\gamma+1}}{16\alpha} \left( \frac{\xi}{\Omega} \right)^{1/2} \right) \quad (\text{heavy particles}) \quad (142)$$

where  $\chi$  is the function defined by equation (131). When  $\xi \rightarrow \infty$ , equation (141) tends to

$$\Omega t_{esc} = \frac{\sqrt{\gamma+1}}{4\alpha} \simeq 200 \quad (143)$$

Very light particles are not concentrated in the vortices and they diffuse away after only  $\sim 30$  rotation periods. This is the *minimum* escape time. By contrast, for optimal particles with  $\xi \sim \Omega$ , the concentration reduces considerably the evaporation and we find

$$\Omega t_{esc} = \frac{4}{3} \frac{\xi}{\Omega} \chi \left( \frac{3\sqrt{\gamma+1}}{16\alpha} \right) \sim 10^{64} \quad (144)$$

The particles are so much concentrated in the vortices ( $l_d \sim 0.1R$ ) that the turbulent fluctuations are not sufficient to allow them to reach the edge of the vortex. Therefore,



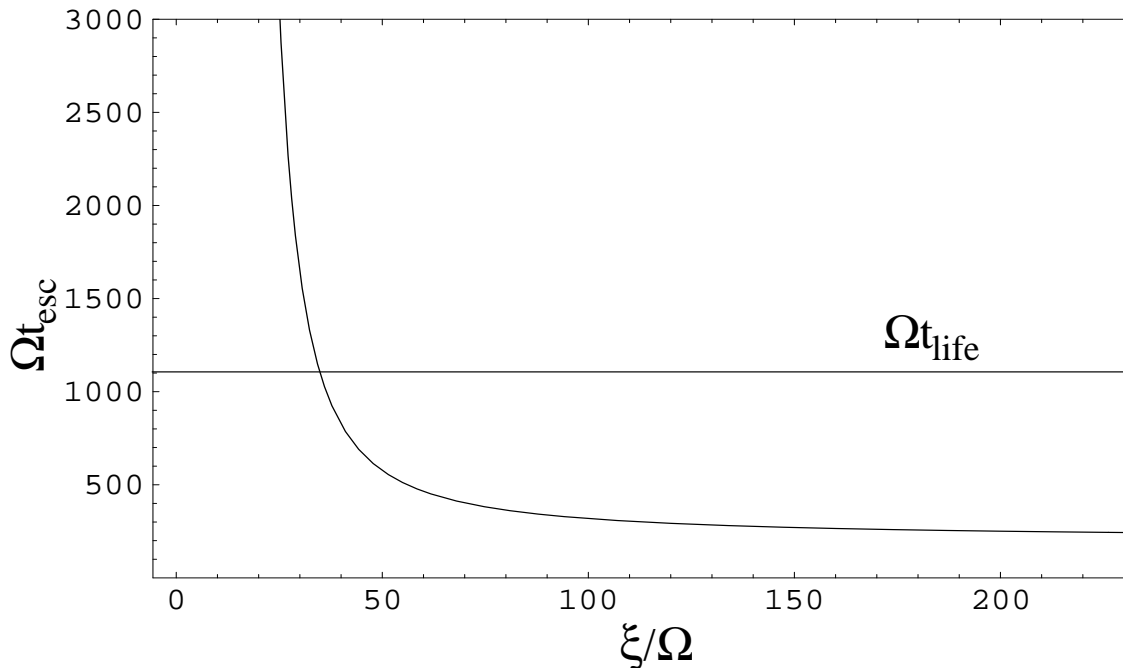


Figure 12: Escape time of the particles as a function of their friction parameter.

their escape is completely negligible. Finally, for  $\xi \rightarrow 0$ , we have

$$\Omega t_{esc} = \frac{\sqrt{\gamma+1}}{4\alpha} \left( \frac{\Omega}{\xi} \right)^{1/2} \quad (145)$$

For very heavy particles, the escape time goes to infinity because the particles are not coupled to the gas and therefore not affected by diffusion. Recall, however, that our study is not well suited for very heavy particles. As discussed in section 2.3, these particles are more likely to cross the vortices without being captured. The curve  $\Omega t_{esc}$  versus  $\xi/\Omega$  is plotted on figure 12 (see also figure 13 for the dependence of  $\Omega t_{esc}$  on the size of the particles). The asymptotic regimes (143) and (145) are obtained for particles with  $\xi/\Omega > 153$  and  $\xi/\Omega < 4 \cdot 10^{-5}$  respectively. For these particles,  $l_d > R$  (see inequalities (75) and (76)), so there is no concentration. Therefore, the asymptotic limits (143) and (145) agree with the results (102) and (103) obtained when the drift term is ignored.

These results assume that there is no renewal of the particles in the vortices. If we now take into account a capture process like in section 2.4, we are led to consider the balance equation:

$$\frac{dM}{dt} = \frac{3}{2} \sigma_d \Omega R^2 f^2(\xi) - \frac{1}{t_{esc}} M \quad (146)$$

The first term in the r.h.s accounts for a flux of particles inside the vortex (see equation (37)) and the second term for an exponential decay of the particle number due to “evaporation” (see equation (138)).

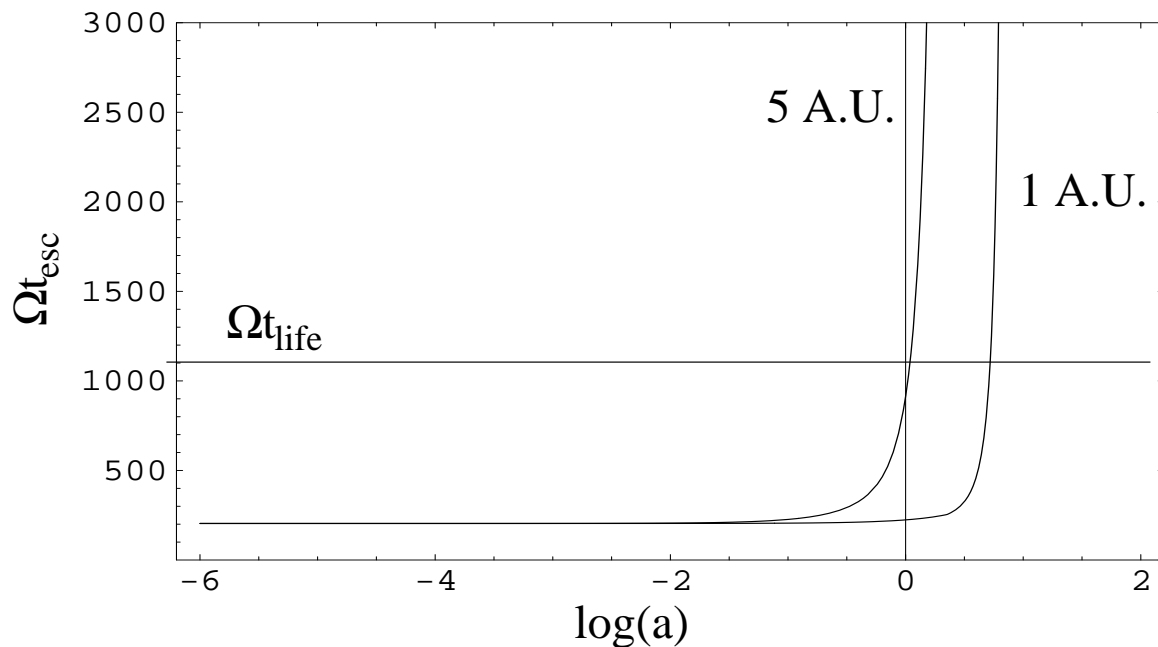


Figure 13: Escape time of the particles as a function of their size at  $r = 1A.U$  and  $r = 5A.U$  ( $\rho_s = 2g/cm^3$ ).

For particles which can experience gravitational collapse (see inequalities (81)(83) and (85)), the escape time is much longer than the vortex lifetime (see figure 12). In that case, evaporation can be neglected and equation (146) reduces to equation (37). The maximum mass captured by the vortex is determined by its lifetime and the results of sections 2.5 and 3.4 are unchanged.

Consider, however, the idealistic situation when  $t_{life} \rightarrow \infty$  (recall that we don't know precisely the value of  $t_{life}$ ). For sufficiently large times ( $t > t_{esc}$ ), the vortex will achieve a stationary distribution of dust particles obtained by setting  $dM/dt = 0$  in equation (146). This gives a maximum mass

$$M_{max} = \frac{3}{2}\sigma_d(\Omega t_{esc})R^2 f^2(\xi) \quad (147)$$

which is now limited by the evaporation time (compare equation (147) with equation (38)). The density enhancement in the vortices (taking into account the concentration effect) is

$$\left(\frac{\sigma_d^{vort}}{\sigma_d}\right)_\infty = \frac{3}{2\pi}(\Omega t_{esc})f^2(\xi)\left(\frac{R}{l_d}\right)^2 \quad (148)$$

as represented on figure 14. We find that even if the vortex had an infinite lifetime, particles with friction parameter  $\xi/\Omega > 30$  cannot trigger the gravitational instability. This result implies (see figure 5) that subcentimetric particles cannot form planetesimals even in the most optimistic case. Sticking processes are necessary to produce larger particles.

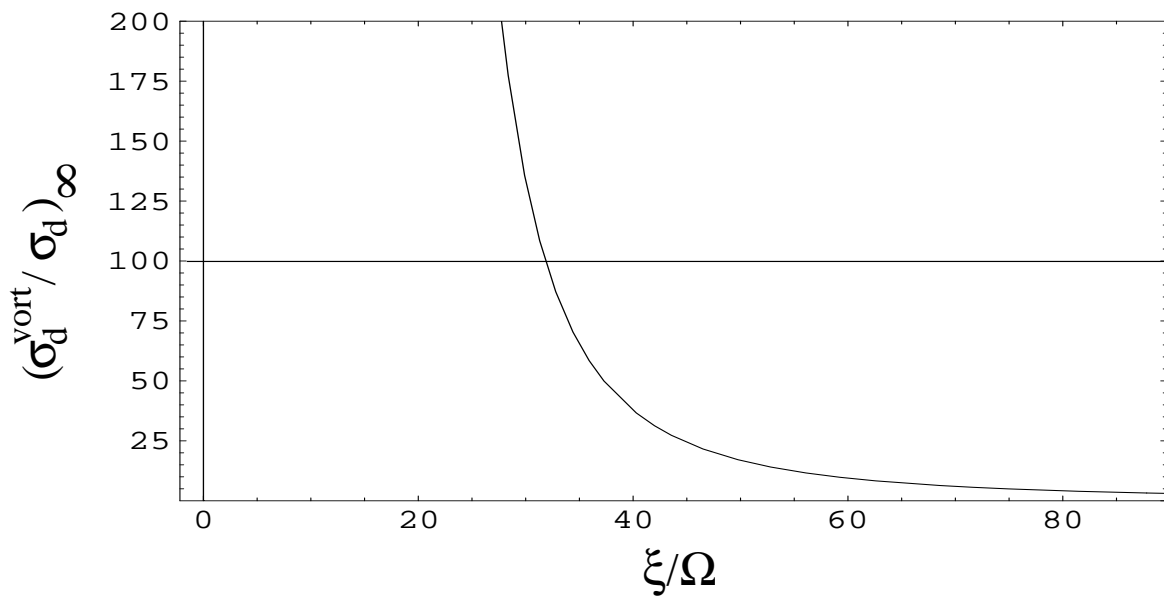


Figure 14: Enhancement of the dust surface density in the vortices as a function of the friction parameter when evaporation due to small scale turbulence is taken into account ( $t_{life} \rightarrow \infty$ ).

## 5 Conclusion

This article follows the works of Barge & Sommeria (1995), Tanga *et al.* (1996), Bracco *et al.* (1999) and Godon & Livio (1999c) concerning the interaction between dust particles and large-scale vortices in the solar nebula. The originality of our study was to start from an exact and realistic solution of the fluid equations and to provide analytical results and relevant parameters for the trapping process. Moreover, we have considered for the first time the effect of small-scale turbulent fluctuations on the motion of the particles and determined an explicit expression for the escape time by solving a problem of quantum mechanics. These theoretical results have been formulated in the context of Keplerian disks and planet formation but they can clearly have applications in other fields of astrophysics and geophysics, for example the transport of pollutants in the Earth's atmosphere.

The vortex scenario provides an attractive mechanism to form planetesimals on very short time scales. This does not contradict the overall picture of planet formation which has been developed over the last decades. On the contrary, it fills the gap between two domains which were difficult to connect: *sticking processes* are still necessary to produce centimetric particles and *collision between planetesimals* is of course the main engine of planet's growth. In between, the vortex scenario should come at work to facilitate, at some preferred locations of the disk, the Safronov-Goldreich-Ward instability which was proposed initially for forming planetesimals.

The predictions of the vortex model are remarkably consistent with the structure of the solar system. The capture process is optimal at two preferred locations of the nebula which correspond, for relevant sizes of the particles (i.e some centimeters), to the position of telluric and giant planets. The transition between the two groups of planets happens to coincide with the passage from the Stokes to the Epstein regime where the gas drag law changes. The asymmetry between the two optima may be ascribed to the size of the vortices which are bigger in the outer zone.

Of course, the results discussed here rely upon the existence of vortices in the disk. Their presence in the solar nebula is reasonable due to the ubiquitous appearance of vortices in rotating flows and two-dimensional turbulence. However, numerical simulations and even laboratory experiments are necessary to ascertain their existence in Keplerian flows. A first step was undertaken by Bracco *et al.* (1998,1999) and Godon & Livio (1999a,b,c) who observed the formation of anticyclones developing from an energetic random initial vorticity field in a Keplerian flow. More work remains to be done to understand the generation (and maintenance) of vorticity in such disks (convection, baroclinic instability...) and to determine the effect of three-dimensionality (Hodgson & Brandenburg 1998) on the stability of these vortices.

## 6 Acknowledgments:

I would like to thank P. Barge and J. Sommeria for introducing me to this fascinating subject and for several illuminating comments. I acknowledge also very stimulating discussions with A. Provenzale, A. Bracco, P. Tanga and E. Spiegel. This work was initiated during my postdoctoral stay at the Istituto di Cosmogeofisica.

## A Elliptic vortex in a uniform shear

In his monograph, Saffman (1992) reports the existence of an exact solution of the incompressible two-dimensional Euler equation consisting of an elliptic patch of uniform vorticity  $\omega$  embedded in a simple shear  $\kappa$ . Since this vortex solution is the starting point of our study, we establish in this appendix the condition (13) for its existence and construct the corresponding streamfunction. These results will be useful for subsequent studies.

First, we introduce a cartesian system of coordinates and write the shear under the form

$$u_x = \kappa y \quad (149)$$

$$u_y = 0 \quad (150)$$

where  $\kappa$  is a constant ( $\kappa = \frac{3}{2}\Omega$  for the Keplerian shear considered in section 2.2). The associated vorticity is  $\omega_{ext} = -\kappa$ .

Inside the vortex, the velocity field can be written

$$u_x = -\frac{q^2}{1+q^2}\omega y \quad (151)$$

$$u_y = \frac{1}{1+q^2}\omega x \quad (152)$$

where  $q = a/b$  is the aspect ratio of the elliptic patch ( $a$  and  $b$  denote the semi-axis in the  $x$  and  $y$  directions respectively) and  $\omega$  the vorticity. We can check that the fluid particles move at constant angular velocity  $\frac{q}{1+q^2}\omega$  along concentric ellipses with aspect ratio  $q$ .

For an incompressible two-dimensional flow, it is convenient to introduce a streamfunction  $\psi$  defined by  $\mathbf{u} = -\hat{\mathbf{z}} \wedge \nabla \psi$  (where  $\hat{\mathbf{z}}$  is a unit vector normal to the flow). For a given vorticity field, the streamfunction is solution of the Poisson equation

$$\Delta \psi = -\omega \quad (153)$$

Inside the vortex, we find that

$$\psi = -\frac{1}{2} \frac{\omega}{1+q^2} (x^2 + q^2 y^2) \quad (154)$$

where we have taken, by convention,  $\psi = 0$  at the centre of the vortex. On the vortex boundary, the streamfunction is constant with value:

$$\psi_0 = -\frac{1}{2} \frac{\omega}{1+q^2} a^2 \quad (155)$$

Outside the vortex, we have to solve the Poisson equation

$$\Delta \psi = \kappa \quad (156)$$

with boundary conditions at infinity

$$\frac{\partial \psi}{\partial x} \rightarrow 0, \frac{\partial \psi}{\partial y} \rightarrow \kappa y \quad \text{for } x, y \rightarrow \infty \quad (157)$$

These boundary conditions insure a continuous matching with the shear (149)(150) at large distances. Introducing the decomposition

$$\psi = \phi + \frac{1}{2}\kappa y^2 \quad (158)$$

the problem (156)(157) is equivalent to solving the Laplace equation

$$\Delta\phi = 0 \quad (159)$$

with boundary conditions at infinity

$$\frac{\partial\phi}{\partial x} \rightarrow 0, \frac{\partial\phi}{\partial y} \rightarrow 0 \quad \text{for } x, y \rightarrow \infty \quad (160)$$

At this stage, we find it convenient to use elliptic coordinates

$$x = c \cosh \xi \cos \eta \quad (161)$$

$$y = c \sinh \xi \sin \eta \quad (162)$$

with  $0 \leq \xi < \infty$  and  $0 \leq \eta < 2\pi$ . The vortex boundary is an ellipse with parameter  $\xi_0$  satisfying

$$\frac{x^2}{c^2 \cosh^2 \xi_0} + \frac{y^2}{c^2 \sinh^2 \xi_0} = 1 \quad (163)$$

This relation determines the semi-axis  $a$  and  $b$  of the ellipse in terms of  $\xi_0$  and  $c$ :

$$a = c \cosh \xi_0 \quad b = c \sinh \xi_0 \quad (164)$$

Alternatively, we have

$$\tanh \xi_0 = \frac{b}{a} = \frac{1}{q} \quad c^2 = a^2 - b^2 \quad (165)$$

In terms of elliptic coordinates the Laplace equation (159) has the simple form

$$\frac{\partial^2\phi}{\partial\xi^2} + \frac{\partial^2\phi}{\partial\eta^2} = 0 \quad (166)$$

This equation, with the boundary condition (160), is solved easily and we obtain outside the vortex

$$\psi = \frac{1}{2}\kappa y^2 + B\xi + \sum_{n=0}^{+\infty} A_n e^{-n\xi} \cos(n\eta + \gamma_n) \quad (167)$$

where  $B$ ,  $A_n$  and  $\gamma_n$  are some constants. At large distances,  $\xi \rightarrow \ln r$  and  $\eta \rightarrow \theta$  (where  $r$  and  $\theta$  are polar coordinates) and we recover the usual multipolar expansion of the streamfunction. The condition that the vortex boundary is a streamline destroys most of the terms in the series (167). There remains only

$$\begin{aligned} \psi = & \frac{\kappa c^2}{4} \sinh^2 \xi (1 - \cos(2\eta)) \\ & + B\xi + A_0 + \frac{\kappa b^2}{4} e^{2(\xi_0 - \xi)} \cos(2\eta) \end{aligned} \quad (168)$$

In addition, the continuity of  $\psi$  on the vortex boundary requires that  $A_0$  and  $B$  be related by

$$-\frac{1}{2} \frac{\omega}{1+q^2} a^2 = \frac{1}{4} \kappa b^2 + B \xi_0 + A_0 \quad (169)$$

We must also satisfy the continuity of the tangential velocity  $\frac{\partial \psi}{\partial \xi}$  at the contact with the vortex. To that purpose, we need first to express the streamfunction (154) inside the vortex in terms of elliptic coordinates. We find:

$$\psi = -\frac{1}{2} \frac{\omega}{1+q^2} c^2 (\cosh^2 \xi \cos^2 \eta + q^2 \sinh^2 \xi \sin^2 \eta) \quad (170)$$

Then, after some algebra, we find that the continuity of the velocity is satisfied provided that

$$\frac{\kappa}{\omega} = \frac{q(1-q)}{1+q^2} \quad (171)$$

and

$$B = -\frac{1}{2} (\kappa + \omega) q b^2 \quad (172)$$

The relations (172) and (169) just determine the constants  $A_0$  and  $B$  appearing in the expression (168) of the streamfunction. In addition, the condition (171) must be satisfied for a solution to exist. In a given shear, equation (171) imposes a relation between the vorticity and the aspect ratio of the vortex.

Regrouping all the results, we find that the streamfunction can be expressed inside the vortex ( $\xi \leq \xi_0$ ) by:

$$\psi_{in} = \frac{\kappa b^2}{2q} (q+1) (\cosh^2 \xi \cos^2 \eta + q^2 \sinh^2 \xi \sin^2 \eta) \quad (173)$$

and outside the vortex ( $\xi \geq \xi_0$ ) by:

$$\begin{aligned} \psi_{out} = & \frac{\kappa}{4} b^2 (q^2 - 1) \sinh^2 \xi (1 - \cos(2\eta)) \\ & + \frac{1}{4} b^2 \kappa \frac{q+1}{q-1} + \frac{1}{2} b^2 \kappa \frac{q+1}{q-1} (\xi - \xi_0) \\ & + \frac{\kappa b^2}{4} e^{2(\xi_0 - \xi)} \cos(2\eta) \end{aligned} \quad (174)$$

## B Gravitational instability of a turbulent rotating disk

In this appendix, we derive an instability criterion for a turbulent rotating disk in the approximation where the disk is a sheet of zero thickness with constant mean density  $\bar{\sigma}$  and constant angular velocity  $\Omega$ . Our study is inspired by the work of Chandrasekhar (1951) concerning the stability of an infinite homogeneous turbulent medium. To our knowledge, the results presented in this appendix are new.

The analysis is easiest if we work in a rotating frame of reference. The equations of the problem are provided by the equation of continuity, the equation of motion and Poisson equation:

$$\frac{\partial \sigma}{\partial t} + \frac{\partial}{\partial x_i} (\sigma u_i) = 0 \quad (175)$$

$$\begin{aligned} \frac{\partial}{\partial t}(\sigma u_i) + \frac{\partial}{\partial x_j}(\sigma u_i u_j) &= -\frac{\partial p}{\partial x_i} - 2\Omega\sigma u_{\perp i} \\ &\quad + \sigma\Omega^2 x_i - \sigma \frac{\partial\Phi}{\partial x_i} \end{aligned} \quad (176)$$

$$\Delta\Phi = 4\pi G\sigma\delta(z) \quad (177)$$

The symbols have their usual meaning and  $\mathbf{u}_{\perp}$  is the vector  $\mathbf{u}$  rotated by  $\frac{\pi}{2}$ . The velocity field  $u_i = (u_x, u_y)$  is purely two-dimensional and, in equations (175)(176), there is summation over repeated indices. In equation (177), the  $\delta$ -function insures that the disk is infinitely thin.

We assume that the disk is turbulent and write

$$\sigma = \bar{\sigma} + \delta\sigma, \quad p = \bar{p} + \delta p, \quad \Phi = \bar{\Phi} + \delta\Phi \quad (178)$$

where  $\bar{\sigma}$ ,  $\bar{p}$  and  $\bar{\Phi}$  are certain constants. With the further assumption that the disk is barotropic, i.e  $p = p(\sigma)$ , we have

$$\frac{\partial p}{\partial x_i} = c_s^2 \frac{\partial\sigma}{\partial x_i} \quad (179)$$

where  $c_s = (dp/d\sigma)^{1/2}$  denotes the velocity of sound. Then, we invoke Jeans swindle (see, e.g. Binney & Tremaine, 1987) to eliminate the centrifugal term, i.e we write

$$\frac{\partial\Phi}{\partial x_i} - \Omega^2 x_i = \frac{\partial\delta\Phi}{\partial x_i} \quad (180)$$

This process is permissible if we assume that the centrifugal force is balanced by a gravitational force that is produced by some unspecified mass distribution (recall that for an infinite uniform disk,  $\nabla\bar{\Phi}$  is necessarily vertical and cannot, by itself, compensate the centrifugal force). In our situation, the external force is provided by the sun's gravity. With the further approximation

$$\sigma \frac{\partial\delta\Phi}{\partial x_i} = (\bar{\sigma} + \delta\sigma) \frac{\partial\delta\Phi}{\partial x_i} \simeq \bar{\sigma} \frac{\partial\delta\Phi}{\partial x_i} \quad (181)$$

the equations of the problem become

$$\frac{\partial\sigma}{\partial t} + \frac{\partial}{\partial x_i}(\sigma u_i) = 0 \quad (182)$$

$$\frac{\partial}{\partial t}(\sigma u_i) + \frac{\partial}{\partial x_j}(\sigma u_i u_j) = -c_s^2 \frac{\partial\sigma}{\partial x_i} - 2\Omega\sigma u_{\perp i} - \bar{\sigma} \frac{\partial\delta\Phi}{\partial x_i} \quad (183)$$

$$\Delta\delta\Phi = 4\pi G\delta\sigma\delta(z) \quad (184)$$

From the continuity equation (182), we readily establish that

$$\frac{\partial}{\partial t} \overline{\sigma\sigma'} = -\frac{\partial}{\partial x_i} \overline{\sigma'\sigma u_i} - \frac{\partial}{\partial x'_i} \overline{\sigma\sigma' u'_i} \quad (185)$$



where  $\sigma$  and  $\sigma'$  are the values of the surface density in  $\mathbf{x}$  and  $\mathbf{x}'$  respectively. We introduce the correlation function of the density fluctuations, defined by:

$$C(\xi, t) = \overline{\delta\sigma\delta\sigma'} = \overline{(\sigma - \bar{\sigma})(\sigma' - \bar{\sigma})} = \overline{\sigma\sigma'} - \bar{\sigma}^2 \quad (186)$$

In homogeneous and isotropic turbulence,  $C(\xi, t)$  is a scalar function depending, apart from time, only on the relative distance  $\xi = |\mathbf{x}' - \mathbf{x}|$  between the points under consideration. Similarly, we define the quantity

$$L_i(\xi, t) = \overline{\sigma'\sigma u_i} = -\overline{\sigma\sigma' u'_i} \quad (187)$$

and set

$$\boldsymbol{\xi} = \mathbf{x}' - \mathbf{x} \quad (188)$$

Remembering that  $\partial/\partial x'_i = -\partial/\partial x_i = \partial/\partial \xi_i$ , we can rewrite equation (185) under the form

$$\frac{\partial C}{\partial t} = 2\nabla_{\boldsymbol{\xi}} \mathbf{L} \quad (189)$$

An equation of motion for  $\mathbf{L}(\xi, t)$  can be derived in the following manner. From equations (182) and (183), it is easy to establish that

$$\begin{aligned} & \frac{\partial}{\partial t} \overline{\sigma'\sigma u_i} + \frac{\partial}{\partial x'_j} \overline{\sigma\sigma' u_i u'_j} + \frac{\partial}{\partial x_j} \overline{\sigma'\sigma u_i u_j} \\ &= -c_s^2 \frac{\partial \overline{\sigma'\sigma}}{\partial x_i} - \bar{\sigma} \frac{\partial \overline{\sigma'\delta\Phi}}{\partial x_i} - 2\Omega \overline{\sigma'\sigma u_{\perp i}} \end{aligned} \quad (190)$$

or, with more convenient notations

$$\frac{\partial L_i}{\partial t} + \frac{\partial}{\partial \xi_j} \overline{\sigma\sigma'(u_i u'_j - u_i u_j)} = c_s^2 \frac{\partial C}{\partial \xi_i} + \bar{\sigma} \frac{\partial \psi}{\partial \xi_i} - 2\Omega L_{\perp i} \quad (191)$$

where we have written

$$\psi = \overline{\sigma'\delta\Phi} = \overline{\delta\sigma'\delta\Phi} \quad (192)$$

The correlation function  $\psi$  is related to  $C$  by the Poisson equation

$$\Delta\psi = 4\pi GC\delta(z) \quad (193)$$

Equations (189) (191) and (193) are perfectly general but the system is not closed since the evolution of  $\mathbf{L}(\xi, t)$  involves the fourth-order correlation functions  $\overline{\sigma\sigma' u_i u'_j}$  and  $\overline{\sigma\sigma' u_i u_j}$  which are not known. To go further, we shall suppose that these fourth-order correlations can be expressed in terms of the second-order correlations as in a joint gaussian distribution. For our purposes, this approximation is reasonable and should provide ample accuracy. Then, by virtue of Wick's theorem, we have:

$$\begin{aligned} \overline{\sigma\sigma' u_i u_j} &= \overline{\sigma\sigma'} \overline{u_i u_j} + \overline{\sigma u_i} \overline{\sigma' u_j} + \overline{\sigma u_j} \overline{\sigma' u_i} \\ &= \overline{\sigma\sigma'} \frac{1}{2} u^2 \delta_{ij} \end{aligned} \quad (194)$$

$$\begin{aligned}\overline{\sigma\sigma'u_iu'_j} &= \overline{\sigma\sigma'} \overline{u_iu'_j} + \overline{\sigma u_i} \overline{\sigma'u'_j} + \overline{\sigma u'_j} \overline{\sigma'u_i} \\ &= \overline{\sigma\sigma'} \overline{u_iu'_j} - \overline{\sigma u'_i} \overline{\sigma'u'_j}\end{aligned}\quad (195)$$

With the foregoing substitution, equation (191) becomes

$$\begin{aligned}\frac{\partial L_i}{\partial t} + \frac{\partial}{\partial \xi_j} [\overline{\sigma\sigma'} \overline{u_iu'_j} - \overline{\sigma u'_i} \overline{\sigma'u'_j}] &= (c_s^2 + \frac{\overline{u^2}}{2}) \frac{\partial C}{\partial \xi_i} \\ &+ \overline{\sigma} \frac{\partial \psi}{\partial \xi_i} - 2\Omega L_{\perp i}\end{aligned}\quad (196)$$

For sufficiently large values of  $\xi$ , the terms in the velocity correlations in equation (196) will become negligible and equation (196) will tend to

$$\frac{\partial \mathbf{L}}{\partial t} = (c_s^2 + \frac{\overline{u^2}}{2}) \nabla_{\xi} C + \overline{\sigma} \nabla_{\xi} \psi - 2\mathbf{\Omega} \wedge \mathbf{L}\quad (197)$$

Equations (189)(197) and (193) are mathematically similar to the linearized equations which appear in the usual problem of Jeans instability for a thin rotating disk (see, e.g, Binney & Tremaine 1987). However, their physical meaning is different since equations (189)(197) and (193) have been derived explicitly from the analysis of the correlations in a turbulent medium.

These equations admit sound waves of the form

$$C = \hat{C} e^{-i\omega t} J_0(k\xi)\quad (198)$$

$$\mathbf{L} = \hat{\mathbf{L}} e^{-i\omega t} J_0(k\xi)\quad (199)$$

$$\psi = \hat{\psi} e^{-i\omega t} J_0(k\xi) e^{-k|z|}\quad (200)$$

where  $J_0$  is Bessel function of order zero. The solution (200) satisfies the Laplace equation  $\Delta\psi = 0$  for  $z \neq 0$  [see equation (193)]. In the plane  $z = 0$ , we have  $\psi = \hat{\psi} e^{-i\omega t} J_0(k\xi)$ . Equation (193) implies that  $\hat{\psi}$  must be related to  $\hat{C}$  in a special manner. To see that, we integrate the Poisson equation from  $-\zeta$  to  $+\zeta$  (where  $\zeta$  is a positive constant) and let  $\zeta \rightarrow 0$ . Since  $\frac{\partial^2 \psi}{\partial x^2}$  and  $\frac{\partial^2 \psi}{\partial y^2}$  are continuous at  $z = 0$ , but  $\frac{\partial^2 \psi}{\partial z^2}$  is not, we have:

$$\begin{aligned}\lim_{\zeta \rightarrow 0} \int_{-\zeta}^{\zeta} \frac{\partial^2 \psi}{\partial z^2} dz &= \lim_{\zeta \rightarrow 0} \left[ \frac{\partial \psi}{\partial z} \right]_{-\zeta}^{\zeta} \\ &= 4\pi G C \int_{-\zeta}^{\zeta} \delta(z) dz = 4\pi G C\end{aligned}\quad (201)$$

Hence  $-2k\psi = 4\pi G C$ , or

$$\hat{\psi} = -\frac{2\pi G \hat{C}}{k}\quad (202)$$

Substituting for  $C$ ,  $\mathbf{L}$  and  $\psi$  in equations (189)(197) and (193), we obtain

$$-i\omega C = 2\frac{1}{\xi} \frac{\partial}{\partial \xi} (\xi L_{\xi})\quad (203)$$

$$-i\omega L_\xi = (c_s^2 + \frac{\overline{u^2}}{2}) \frac{\partial C}{\partial \xi} + \overline{\sigma} \frac{\partial \psi}{\partial \xi} + 2\Omega L_\eta \quad (204)$$

$$-i\omega L_\eta = -2\Omega L_\xi \quad (205)$$

where  $\xi, \eta$  are polar coordinates. Eliminating  $L_\eta$  between (204) and (205) yields

$$\frac{\omega^2 - 4\Omega^2}{i\omega} L_\xi = (c_s^2 + \frac{\overline{u^2}}{2}) \frac{\partial C}{\partial \xi} + \overline{\sigma} \frac{\partial \psi}{\partial \xi} \quad (206)$$

Substituting the foregoing expression for  $L_\xi$  into equation (203), we arrive at

$$(4\Omega^2 - \omega^2)C = 2(c_s^2 + \frac{\overline{u^2}}{2})\Delta_\xi C + 2\overline{\sigma}\Delta_\xi \psi \quad (207)$$

Using the expressions (198) (200) (202) for  $C$  and  $\psi$  and remembering that  $J_0(k\xi)$  is an eigenfunction of the two-dimensional Laplacian operator with eigenvalue  $-k^2$ , we obtain the dispersion relation

$$\omega^2 = 4\Omega^2 + 2 \left[ k^2 (c_s^2 + \frac{\overline{u^2}}{2}) - 2\pi G \overline{\sigma} k \right] \quad (208)$$

This result differs from the usual dispersion relation (77) in the occurrence of  $c_s^2 + \frac{\overline{u^2}}{2}$  in place of  $c_s^2$  and by a factor 2. Similar differences with the usual Jeans dispersion relation were noticed by Chandrasekhar (1951) in his analysis of an infinite homogeneous turbulent medium.

The function  $\omega^2(k)$  is quadratic in  $k$  with a minimum at  $k_c = \pi G \overline{\sigma} / (c_s^2 + \frac{\overline{u^2}}{2})$ . The disk will be unstable to some wavelengh  $k^{-1}$  provided that  $\omega^2(k_c) < 0$ , i.e:

$$\sqrt{2 \left( c_s^2 + \frac{\overline{u^2}}{2} \right)} < \frac{\pi G \overline{\sigma}}{\Omega} \quad (209)$$

This is the generalisation of the Toomre instability criterion (78) in the case where the disk is turbulent. For a real disk, with finite thickness  $H$ ,  $\frac{\overline{u^2}}{2}$  should be replaced by  $\frac{\overline{u^2}}{3}$  since small-scale fluctuations are basically three-dimensional. When the turbulent dispersion  $c_{turb} = \sqrt{\overline{u^2}}$  dominates over the sound velocity, as it is the case in our study, we obtain

$$c_{turb} < \frac{\pi G \overline{\sigma}}{\Omega} \quad (210)$$

This result justifies the procedure used in section 3.4 of replacing the sound velocity occurring in equation (78) by the more relevant turbulent dispersion of the particles. However, in more general situations, the turbulent dispersion needs not be large compared to the velocity of sound and the criterion (209) should be used.

## References

- [1] Abramowicz M.A., Lanza A., Spiegel E.A. & Szuskiewicz E. 1992, *Nat* 356, 41
- [2] Adams F.C & Watkins R. 1995, *ApJ* 451, 314
- [3] Balbus S.A. & Hawley J.F. 1991, *ApJ* 376 214
- [4] Balbus S.A., Hawley J.F. & Stone J.M. 1996, *ApJ* 467 , 76
- [5] Barge P. & Pellat R. 1991, *Icarus* 93, 270
- [6] Barge P. & Pellat R. 1993, *Icarus* 104 79
- [7] Barge P. & Sommeria J. 1995, *A&A* 295, L1
- [8] Bengtson L. & Lighthill M.J. 1982, *Intense Atmospheric Vortices*, Springer-Verlag
- [9] Binney J. & Tremaine S. 1987, *Galactic Dynamics*, Princeton Series in Astrophysics
- [10] Bracco A., Chavanis P.H., Provenzale A. & Spiegel E.A. 1999, *Phys. Fluids* 11, 2280
- [11] Bracco A., Provenzale A., Spiegel E.A. & Yecko P., *Proceedings of the Conference on Quasars and Accretion Disks*, ed. M. Abramowicz, Cambridge Univ. Press 1998
- [12] Cabot W., Canuto V.M., Hubickyj O. & Pollack J.B. 1987a, *Icarus* 69, 387
- [13] Cabot W., Canuto V.M., Hubickyj O. & Pollack J.B. 1987b, *Icarus* 69, 423
- [14] Chandrasekhar S. 1943a, *Rev. Mod. Phys.* 15, 1
- [15] Chandrasekhar S. 1943b, *ApJ.* 97, 263
- [16] Chandrasekhar S. 1946, *Rev. Mod. Phys.* 18, 94
- [17] Chandrasekhar S. 1949, *ApJ* 110, 329
- [18] Chandrasekhar S. 1951, *Proc. Roy. Soc. A* 210, 26
- [19] Chavanis P.H. 1996, *Thèse de doctorat*, Ecole Normale Supérieure de Lyon
- [20] Chavanis P.H., Sommeria J. & Robert R. 1996, *ApJ* 471, 385
- [21] Chavanis P.H. 1998a, *Ann. N. Y. Acad. Sci.* 867, 120-141
- [22] Chavanis P.H. 1998b, *Formation des planètes à l'intérieur de tourbillons organisés dans la nébuleuse primordiale*. In: *Ecole thématique d'Arc 2000, Aux frontières de la dynamique chaotique des systèmes gravitationnels*, Observatoire de la Côte d'Azur
- [23] Chavanis P.H. & Sommeria J. 1998, *J. Fluid Mech.* 356, 259

- [24] Chavanis P.H. 1999, From Jupiter's Great Red Spot to the structure of galaxies: statistical mechanics of two-dimensional vortices and stellar systems. In: Ecole thématique de Pralognan, Interrelation entre la physique et la dynamique des systèmes gravitationnels, Observatoire de la Côte d'Azur
- [25] Cuzzi J.N., Dobrovolskis A.R. & Champney J.M. 1993, *Icarus* 106, 102
- [26] Descartes 1643, *Principia Philosophiae*
- [27] Dowling T.E. & Spiegel E.A. 1990, *Ann. N.Y. Acad. Sci.* 617, 190
- [28] Dubrulle B. & Frisch U. 1991, *Phys. Rev. A* 243, 5355
- [29] Dubrulle B. 1992, *A&A* 266, 592
- [30] Dubrulle B. & Knobloch E. 1992, *A&A* 256, 673
- [31] Dubrulle B. & Valdetaro L. 1992, *A&A* 263, 387
- [32] Dubrulle B. 1993, *Icarus* 106, 59
- [33] Dubrulle B., Morfill G. & Sterzik M. 1995, *Icarus* 114, 237
- [34] Frisch U., She Z.S. & Sulem P.L. 1987, *Physica D* 28, 382
- [35] Godon P. & Livio M. 1999a, *ApJ* 521, 319
- [36] Godon P. & Livio 1999b, *ApJ* 523, 350
- [37] Godon P. & Livio M 1999c, astro-ph/9910418
- [38] Goldreich P. & Ward W.R. 1973, *ApJ* 183, 1051
- [39] Graner F. & Dubrulle B. 1994, *A&A* 282, 262
- [40] van Heijst G.J.F. & Flor J.B. 1989, *Nat* 340, 212
- [41] Hodgson L.S. & Brandenburg A. 1998, *A&A* 330, 1169
- [42] Hopfinger E.J., Browand F.K. & Gagne Y., 1983, *J. Fluid Mech.* 125, 505
- [43] Hunter J.H. & Horak T. 1983, *ApJ* 265, 402
- [44] Kant I. 1755, *Algemeine Natur. Theorie des Himmels*, Königsberg
- [45] Kitchatinov L.L., Rüdiger G. & Khomenko G. 1994, *A&A* 287, 320
- [46] Kraichnan R.H. & Montgomery D. 1980, *Rep. Prog. Phys.* 43, 547
- [47] Kramers H.A. 1940, *Physica* 7, 284
- [48] Laplace P.S. 1796, *Exposition du système du monde*, Paris
- [49] Lin D.N.C. & Papaloizou J. 1980, *MNRAS* 191, 37

- [50] Lovelace R.V.E., Li H., Colgate S.A. & Nelson A.F. 1999, *ApJ* 513, 805
- [51] Lynden-Bell D. 1967, *MNRAS* 136, 101
- [52] Marcus P.S. 1990, *J. Fluid Mech.* 215 , 393
- [53] Miller J. 1990, *Phys. Rev. Lett.* 65 ,17, 2137
- [54] Nakagawa Y., Sekiya M. and Hayashi C. 1986, *Icarus* 67, 375
- [55] Nezlin M.V. & Snezhkin E.N. 1993, *Rosby vortices, spiral structures, solitons*. Springer-Verlag
- [56] Robert R. and Sommeria J. 1991, *J. Fluid Mech.* 229, 291
- [57] Saffman P.G. 1992, *Vortex Dynamics*, Cambridge University Press
- [58] Safronov V.S. 1969, *Evolution of the Protoplanetary cloud and formation of the Earth and the planets*, Moscow
- [59] Shakura N.L. & Sunyaev R.A. 1973, *A&A* 24, 337
- [60] Sommerfeld A. & Welker H. 1938, *Ann. d. Phys.* 32, 56
- [61] Sommerfeld A. & Hartmann H. 1940, *Ann. d. Phys.* **37**, 333
- [62] Sommeria J., Meyers S.D. & Swinney H.L. 1988, *Nat* 331, 689
- [63] Sommeria J., Nore C., Dumont T., Robert R. 1991, *C.R. acad. Sci. Paris II* 312 999
- [64] Tanga P., Babiano A., Dubrulle B., Provenzale A. 1996, *Icarus* 121 158
- [65] Toomre A. 1964, *ApJ* 139, 1217-1238
- [66] Völk H.J., Jones F.C., Morfill G.E. & Röser S. 1980, *A&A* 85, 316
- [67] Weidenschilling S.J. 1977, *MNRAS* 180, 57-70
- [68] Weidenschilling S.J. 1980, *Icarus* 44, 172
- [69] Weidenschilling S.J. & Cuzzi J.N., 1993. In Levy, E.H., Luline, J.L., Matthews, M.S. (eds.) *Protostars and Planets III*. Univ. Arizona Press, Tucson, p 1031
- [70] von Weizsäcker C.F. 1944, *Zeit. für Astrophys.* 22, 319
- [71] Wetherill G.W., 1988. In Weaver, H.A., Danly, L., (eds.) *The formation and evolution of planetary systems*. Cambridge Univ. Press, Cambridge, p 344
- [72] McWilliams J.C. 1990, *J.Fluid Mech* 219, 361